Composition and Detection of Europa's Sputter-induced Atmosphere

R. E. Johnson
University of Virginia

M. H. Burger
University of Maryland/NASA Goddard Space Flight Center

T. A. Cassidy
University of Virginia

F. Leblanc
Service d'Aéronomie du Centre National de la Recherce Scientifique

M. Marconi
Prima Basic Research, Inc.

W. H. Smyth
Atmospheric and Environmental Research, Inc.

An intense flux of ions and electrons from the jovian magnetosphere both alters and erodes Europa's surface, producing a tenuous atmosphere. This chapter discusses the physical processes that create and remove the atmosphere, such as ion erosion (sputtering), radiation-induced chemical alteration of the surface (radiolysis), and atmospheric loss processes such as ionization and pickup. Special emphasis is placed on ongoing modeling efforts to connect atmospheric properties to surface composition. Models are at present constrained by a small number of observations, but a future mission to Europa has the potential to detect even trace atmospheric species.

1. INTRODUCTION

Europa has a tenuous atmosphere, which, unlike that of Titan, Io, or Callisto, is only marginally collisional. Because the atmosphere is quasi-collisional, it is often referred to as an exosphere. Alternatively, and more relevant to the present discussion, it is also called a surface boundary-layer atmosphere (*Johnson,* 2002), i.e., as at Mercury, the Moon, and Ganymede, the interaction of the ambient gas with the surface determines its composition, local column density, and morphology. All molecules and atoms in the atmosphere are quickly lost either to space or the surface, and lifetimes are measured in minutes to days, depending on the species. Neutrals that escape Europa's gravity mostly remain gravitationally bound to Jupiter in a toroidal-shaped cloud with peak densities near Europa's orbital path.

Since gas-phase species are readily identified both *in situ* and by remote sensing, Europa's atmosphere is of interest as an extension of its surface. If this atmosphere was only populated by thermal desorption (i.e., evaporation), it would consist only of *trace volatiles* that would be rapidly depleted, plus a small subsolar component, $<\sim 10^{12}$ H_2O/cm^2 depending on the ice fraction in the surface (*Shematovich et al.,* 2005; *Smyth and Marconi,* 2006). However, Europa orbits in a region of the jovian magnetosphere in which the trapped plasma density and temperature are relatively high, and its surface is exposed to the solar EUV flux. This radiation chemically alters and erodes the surface with the ejecta populating the atmosphere, as seen in Fig. 1. These processes are often lumped together using the words sputter-produced atmosphere, by analogy with the industrial process in which gas-phase species are produced from refractory materials by plasma bombardment, but the individual processes are discussed in the following.

Early laboratory sputtering data by Brown, Lanzerotti, and co-workers (e.g., *Brown et al.,* 1982) were used to predict the principal atmospheric component, O_2, and its average column density (*Johnson et al.,* 1982). These predictions were confirmed over a decade later (see chapter by McGrath et al.). Since loss of H_2 accompanies the formation and ejection of O_2 from ice (*Johnson and Quickenden,* 1997) and it escapes more readily than the heavier species, H_2 is the principal species in Europa's neutral torus. There are approximately three times as many molecules and atoms

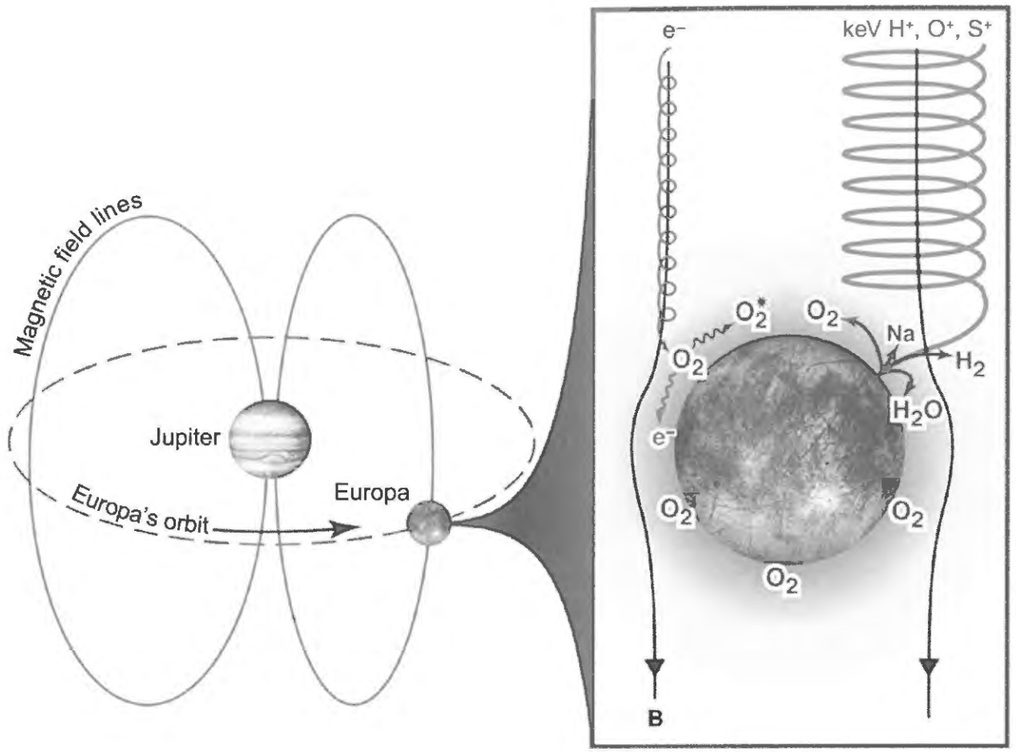

Fig. 1. See Plate 24. Schematic of Europa's interaction with Jupiter's magnetosphere (*Johnson et al.,* 2004). Ions and electrons trapped by Jupiter's magnetic field alter and erode the surface, producing a tenuous atmosphere composed mostly of O_2 with an extended neutral torus of primarily H_2.

in this torus than in Io's neutral torus (*Smyth and Marconi,* 2006). This torus is both a primary source of protons for the jovian magnetosphere and an obstacle to the inward diffusing energetic plasma that significantly affects the properties inside of Europa's orbit (see chapter by Paranicas et al.).

Models for the surface composition, the radiation flux to the surface, and laboratory data have been used in atmospheric simulations in order to interpret the available observations, to refine predictions of Europa's atmospheric structure and composition, and to suggest which sputtered species, other than water products, might be detectable by an orbiting spacecraft. Although the only other neutrals identified to date are sodium and potassium, modeling has shown the importance of the interaction of returning atoms and molecules with Europa's porous regolith (*Leblanc et al.,* 2005; *Cassidy et al.,* 2007), i.e., in a nearly collisionless surface-boundary-layer atmosphere, redistribution and loss to the surface compete with other loss processes such as pick-up (where a newly ionized particle is swept away by the moving magnetospheric plasma), direct escape, and escape of hot (fast) dissociation products. In this chapter we review the modeling of Europa's gravitationally bound atmosphere and neutral cloud. Our principal interest is in the morphology of the atmosphere and the relationship between its composition and Europa's surface composition. The possibility of detection of atmospheric species, either remotely or *in situ* by an orbiting spacecraft, is considered, and their potential relevance to Europa's putative subsurface ocean is discussed.

2. SUMMARY OF PRESENT KNOWLEDGE

2.1. Atmospheric Observations

The first observations of Europa's atmosphere were made by *Hall et al.* (1995) using the Hubble Space Telescope (HST) (see chapter by McGrath et al.). Based on the ratio of atomic oxygen line intensities at 1304 Å and 1356 Å, they concluded that the emissions resulted from electron impact dissociation excitation of O_2 in Europa's atmosphere. Space

Telescope Imaging Spectrometer observations indicated that these emissions were spatially inhomogeneous (*McGrath et al.,* 2004; *Cassidy et al.,* 2007).

The Imaging Science Subsystem on Cassini obtained a series of images of the trailing hemisphere while Europa was in Jupiter's shadow (*Porco et al.,* 2003; see chapter by McGrath et al.). Limb brightening in those images indicated atmospheric emission and the Ultraviolet Imaging Spectrograph (UVIS) detected both hydrogen and oxygen (*Hansen et al.,* 2005). The sharply peaked O I 1356 Å emission line suggested O_2 emission near the surface, while the broader 1304 Å emission line suggested a tenuous extended atomic O component. While no variability was detected in the atmosphere on timescales comparable to the rotation period of Jupiter's magnetic field (10 hours), they did measure intensity differences between observations made six days apart, suggesting temporal variability in the atmosphere or the impacting plasma.

Observations of Europa's ionosphere can constrain both the surface composition and the escape rate, since freshly formed ions are picked-up by the magnetic field and can be swept away (see chapter by Kivelson et al.). The radio signal from the Galileo spacecraft to Earth on the inbound and outbound portions of four occultations showed ionospheric refraction during seven of the eight observation opportunities (*Kliore et al.,* 1997). The ionosphere was found to vary both longitudinally and with Europa's local time (orbital position with respect to the Sun). The maximum electron density of ~10^4 cm^{-3} was observed over the trailing hemisphere. The measured scale height, 240 ± 40 km for alititudes less than 300 km, and 440 ± 60 km for altitudes above 300 km, differed significantly from the 20-km scale height predicted for O_2 (e.g., *Shematovich et al.,* 2005). The nondetection occurred over the downstream hemisphere near the center of the plasma wake. Although not confirmed by modeling, it was suggested that presence of a detectable ionosphere required the trailing (upstream) hemisphere to be partially illuminated. From these observations, Europa has an anisotropic ionosphere with electron densities that reach ~10,000 cm^{-3} near the upstream hemisphere surface.

Using the Galileo PLS instrument, *Paterson et al.* (1999) found maximum ion densities of about 40 cm^{-3} near the closest approach altitudes of 700 km and 600 km on the E4 and E6 flybys. This is several times higher than the average ion densities near Europa's orbit. Pickup ions corresponding to H^+, H_2^+ and mass 16–19 amu (H_2O^+, H_3O^+, OH^+, and O^+ could not be distinguished) were detected downstream of Europa on both flybys. Using the Galileo PWS instrument, strong enhancements in electron density, including a value of 275 cm^{-3} in the downstream wake region during the E11 flyby, were reported (*Kurth et al.,* 2001), as were ion-cyclotron waves associated with pickup ions. Using the Galileo magnetometer, ion-cyclotron waves in Europa's magnetospheric wake were associated with O_2^+, Na^+ and/or Mg^+, Ca^+ and/or K^+, Cl^+, and Cl^- (*Volwerk et al.,* 2001). These ion-cyclotron waves are generated by freshly produced ions in a moving plasma and, since these species were detected near Europa, they are presumably representative of the surface composition.

2.2. Radiation Environment

Properly modeling Europa's atmosphere requires understanding the state of the plasma flowing through it. The undisturbed plasma depends on Europa's position in the Io plasma torus. Because of the 0.13 R_J offset and 9.6° tilt of Jupiter's magnetic dipole, Europa's magnetic coordinate L, defined as the distance from the dipole center that a magnetic field line crosses the magnetic equator, varies from 9.4 R_J to 9.7 R_J as a function of magnetic longitude. In addition, near Europa, plasma is convected back and forth across magnetic field lines as it moves arouud Jupiter by an east-west electric field, and the magnetic field lines are distorted by an azimuthal current sheet centered on the magnetic equator and stretching to ~50 R_J. Therefore, Europa sees a plasma flux that varies with its local time and magnetic (System III) longitude.

Unlike the cooler, denser plasma near Io, the plasma near Europa is too tenuous to produce emissions bright enough for groundbased observations. Using Voyager data, *Bagenal* (1994) produced a two-dimensional model of the plasma that extends to Europa's orbit. At Europa's mean L shell (9.4 R_J), the electrons were described in the centrifugal equator by a cold component with $n_{e,c}$ = 130 cm^{-3} and $T_{e,c}$ = 18 eV and a hot component with $n_{e,h}$ = 3 cm^{-3} and $T_{e,h}$ = 190 eV. Assuming a longitudinally symmetric torus centered on Jupiter's dipole, the electron density varies between ~70 cm^{-3} and 160 cm^{-3} over Jupiter's rotational period. Nondipolar effects and variable plasma sources affect these numbers: Galileo observations show electron densities varying between 18 cm^{-3} and 250 cm^{-3} with a mean value ~200 cm^{-3} in the centrifugal equator (*Moncuquet et al.,* 2002; *Kivelson,* 2004). On its approach to Jupiter, Cassini UVIS observations of the energy content of the Io plasma torus show a 25% variation over two months and shorter brightening events, lasting about 20 hours, with up to 20% variation (*Steffl et al.,* 2004). Since this outwardly diffusing plasma both supplies and removes Europa's atmosphere, the atmospheric content is likely variable, although there are currently no observations that correlate the plasma variability with atmospheric content.

The ion *number density* is dominated by a cold thermal component with a small population of nonthermal "hot" ions. The thermal plasma is primarily singly and doubly ionized oxygen and sulfur with a significant population of hydrogen ions. Near Europa, O^+ and O^{++} dominate, with S^+, S^{++}, and S^{+++} occurring in roughly equal amounts and the S^{+z}/O^{+z} ratio is ~0.2, but variable in time. Because the mean charge state is ~1.5, the ion density is lower than the electron density (*Bagenal,* 1994; *Steffl et al.,* 2004).

In contrast, the plasma ion *energy density* is dominated by an energetic nonthermal component. Energetic ion spectra from 20 keV to 20 MeV were obtained by the Galileo

TABLE 1. Photoreactions* (from *Huebner et al.*, 1992) and electron impact reactions.

Photoreactions		
Reaction	Rate (s^{-1})	
$O + h\nu \rightarrow O^+ + e$	7.8×10^{-9}	
$O_2 + h\nu \rightarrow O + O$	1.6×10^{-7}	
$O_2 + h\nu \rightarrow O_2^+ + e$	1.7×10^{-8}	
$O_2 + h\nu \rightarrow O + O^+ + e$	4.1×10^{-9}	
$Na + h\nu \rightarrow Na^+ + e$	6.0×10^{-7}	
$H + h\nu \rightarrow H^+ + e$	2.7×10^{-9}	
$H_2 + h\nu \rightarrow H + H$	3.0×10^{-9}	
$H_2 + h\nu \rightarrow H_2^+ + e$	2.0×10^{-9}	
$H_2 + h\nu \rightarrow H + H^+ + e$	3.5×10^{-10}	
$H_2O + h\nu \rightarrow OH + H$	3.8×10^{-7}	
$H_2O + h\nu \rightarrow H_2 + O$	2.2×10^{-8}	
$H_2O + h\nu \rightarrow H + H + O$	2.8×10^{-8}	
$H_2O + h\nu \rightarrow H_2O^+ + e$	1.2×10^{-8}	
$H_2O + h\nu \rightarrow H + OH^+ + e$	2.0×10^{-9}	
$H_2O + h\nu \rightarrow OH + H^+ + e$	4.8×10^{-10}	
Electron Impact Reactions		
Reaction	k(20 eV) ($cm^3\ s^{-1}$)	k(250 eV) ($cm^3\ s^{-1}$)
$O + e \rightarrow O^+ + 2e$ [1]	2.2×10^{-8}	1.1×10^{-7}
$O_2 + e \rightarrow O + O + e$ [2]	1.3×10^{-8}	—
$O_2 + e \rightarrow O_2^+ + 2e$ [3]	2.4×10^{-8}	1.1×10^{-7}
$O_2 + e \rightarrow O + O^+ + 2e$ [3]	8.9×10^{-9}	6.1×10^{-8}
$Na + e \rightarrow Na^+ + 2e$ [4]	1.1×10^{-7}	1.0×10^{-7}
$H + e \rightarrow H^+ + 2e$ [5]	1.3×10^{-8}	2.8×10^{-8}
$H_2 + e \rightarrow H + H + e$ [6]	2.7×10^{-10}	1.3×10^{-11}
$H_2 + e \rightarrow H_2^+ + 2e$ [7]	1.6×10^{-8}	4.4×10^{-8}
$H_2 + e \rightarrow H + H^+ + 2e$ [7]	8.1×10^{-10}	3.4×10^{-9}
$H_2O + e \rightarrow OH + H + e$ [8]	3.8×10^{-8}	—
$H_2O + e \rightarrow H_2 + O + e$ [8]	Unknown†	Unknown†
$H_2O + e \rightarrow H_2O^+ + 2e$ [8]	2.3×10^{-8}	8.0×10^{-8}
$H_2O + e \rightarrow H + OH^+ + 2e$ [8]	5.8×10^{-9}	2.6×10^{-8}
$H_2O + e \rightarrow OH + H^+ + 2e$ [8]	3.3×10^{-9}	2.3×10^{-8}

*Assumes Sun is in "quiet" state, normalized to 5.2 AU.
†According to [8], reaction cross sections have not been measured.
References: [1] *Johnson et al.* (2005); [2] *Cosby* (1993); [3] *Straub et al.* (1996); [4] *Johnston and Burrow* (1995); [5] *Shah et al.* (1987); [6] *De La Haye* (2005); [7] *Lindsay and Mangon* (2003); [8] *Itikawa and Mason* (2005).

Energetic Particle Detector (*Cooper et al.*, 2001; *Paranicas et al.*, 2002; chapter by Paranicas et al.) and at higher energies up to 50 MeV/n by the Galileo Heavy Ion Counter (*Cohen et al.*, 2001; *Paranicas et al.*, 2002). The peak flux occurs near 100 keV and diminishes rapidly at higher energies. The high-energy sulfur and oxygen ion components of this flux are primarily responsible for sputtering the surface and producing the atmosphere.

The surface layer altered by the impacting magnetospheric energetic ions and electrons varies from micrometers on short timescales to meters on timescales of a Gigayear (see chapter by Paranicas et al.). Infrared spectrometry typically probes only to a depth of a few micrometers. The surface is also mixed to meter depths by micrometeoroid impacts. The total impacting plasma energy flux is ~8×10^{10} keV/cm^2s, which is comparable to the energy flux due

to tidal and radiogenic sources (*Cooper et al.*, 2001). The energetic component of the plasma flux has been observed to vary by up to a factor of 5, with peak flux around a few tens of keV (*Paranicas et al.*, 2002). At such energies, the rate of ejection of molecules due to S and O ion impacts is ~10 H_2O per ion (*Johnson et al.*, 2004). However, the energetic ion flux is significant out to higher energies, where over 1000 H_2O molecules are ejected per ion giving an average resurfacing rate of 0.01 μm to 0.1 μm per year (or 10 to100 m per G.y.) (*Cooper et al.*, 2001; *Paranicas et al.*, 2002). Although this rate is lower than the resurfacing rate induced by meteoroid gardening, sputtering is the principal source of Europa's atmosphere (*Shematovich et al.*, 2005; *Smyth and Marconi*, 2006).

The energetic electrons and the thermal plasma primarily irradiate the trailing hemisphere of Europa, whereas the energetic ion flux is roughly uniform in longitude and latitude (see chapter by Paranicas et al.). Therefore, the total dose rate at 0.1 mm depth may be 100 times smaller on the leading hemisphere and in polar regions than on the trailing hemisphere. This asymmetry, as well as the preferential bombardment of the trailing hemisphere by low-energy sulfur ions from the Io torus (*Pospeiszalska and Johnson*, 1989), may explain the strong asymmetry in the IR signature of the hydrate observed in Europa's surface (see chapter by Carlson et al.).

Not only does the magnetospheric plasma flux produce an atmosphere, it also removes atmosphere. Atmospheric sputtering by ion-neutral collisions, and dissociation and ionization of atmospheric molecules by low-energy (thermal) electrons, are important loss processes (Table 1) (*Saur et al.*, 1998; *Shematovich et al.*, 2005; *Smyth and Marconi*, 2006). This radiation also makes the atmosphere visible by producing the UV emissions from O_2.

2.3. Surface Composition

Europa's surface composition determines the composition of its atmosphere. The surface is predominantly water ice with impact craters, cracks, ridges, possibly melted regions, and trace species determining how its appearance varies with latitude and longitude (see chapter by Carlson et al.). Due to tidal heating, Europa's surface is relatively young, 20–180 m.y. (*Schenk et al.*, 2004), and material from its putative underground ocean may have reached the surface in its recent past. The trace surface species may also be exogenic — implanted as plasma ions from the jovian magnetosphere, as neutrals or grains from Io, or meteoroid and comet impacts.

The most apparent trace species, sulfur, is preferentially seen on its trailing hemisphere as a brownish tinge in the visible, but is also seen in the cracks and crevices as part of a banded structure. Associated with this feature, reflectance spectra in the UV and near IR suggest the presence of SO_2 inclusions in an ice matrix and a hydrated sulfur-containing species: hydrated sulfuric acid possibly containing hydrated sulfate salts (*McCord et al.*, 1998a,b, 1999, 2001, 2002; chapter by Carlson et al.). Spectral features that appear strongest on the leading hemisphere have been associated with CO_2 trapped in an ice matrix (*Smythe et al.*, 1998). Carbonic acid is also seen, but with a more uniform global distribution. These oxygen-rich sulfur and carbon species are produced by the radiolytic processing of implanted or intrinsic materials (*Johnson et al.*, 2004). Radiolytic processing might also be responsible for the oxidized nature of the surface, e.g., the surface is rich in sulfates instead of sulfides. Radiolysis produces O_2 and H_2 from water ice, and the H_2 leaves the surface more quickly. O_2 also leaves the surface, but some of it stays trapped in the ice matrix (*Johnson and Jesser*, 1997; *Teolis et al.*, 2005; *Hand et al.*, 2006). Radiolysis also produces the observed H_2O_2 and O_3 (*Johnson and Jesser*, 1997; *Johnson and Quickenden*, 1997; *Spencer and Calvin*, 2002; *Cooper et al.*, 2003). Therefore, Europa's surface is dominated by oxygen-rich species. Although radiolysis is a surface oxidizing process, Europa may have been oxidized during formation (*McKinnon and Zolensky*, 2003; see chapter by Zolotov and Kargel).

3. SPUTTERING AND VOLATILE PRODUCTION

3.1. Introduction

Following the Pioneer and Voyager spacecraft encounters with Jupiter and Saturn, *Brown et al.* (1982) and others carried out experiments in which water ice and other low temperature, condensed-gas solids were exposed to energetic ions and electrons. In addition to demonstrating that these solids were chemically altered by the incident radiation, they showed that molecules were ejected into the gas phase with surprising efficiencies, producing the atmospheres eventually observed on Europa and Ganymede. Since those early experiments a considerable amount of laboratory data has been accumulated. There are a number of reviews of the data relevant to the production of the thin atmosphere at Europa (*Johnson*, 1990, 1998, 2001; *Baragiola*, 2003; *Fama et al.*, 2008). In order to model this atmosphere, the sputtering efficiencies for ice by ions, electrons and photons are described, followed by a review of the decomposition and production of O_2 and H_2, the energy spectra of the ejected molecules, and estimates for sputtering of trace species.

3.2. Sputtering Yields

When an energetic ion is incident on an ice surface in a laboratory or in space, molecules are ejected (sputtered) due to both momentum transfer collisions between the incident ion and water molecules in the solid and electronic excitations of these molecules. The relative importance depends on the ion velocity and its charge state. Although the database is considerable (*people.virginia.edu/~rej/sputter_surface.html*), experiments have not been carried out on all ions and energies of interest. In order to understand the physics and chemistry occurring in the solid, the sputtering yield, the number of molecules ejected per incident ion, is typically given in terms of the energy that an ion depos-

its as it passes through a solid, dE/dx, often called the stopping power.

For an energetic ion, dE/dx has two components: one due to the electronic excitation of molecules in the solid, $(dE/dx)_e$, and one due to momentum transfer collisions, written as $(dE/dx)_n$, also called knock-on or elastic nuclear collisions. Since both quantities are proportional to the molecular density, n, one writes: $dE/dx = n\,(S_n + S_e)$. Estimates of S_n and S_e, called the nuclear and electronic stopping cross sections, can be obtained from the freeware program SRIM (*www.srim.org*) (*Ziegler et al.,* 1985). Using these quantities, the sputtering yields for water ice at low temperatures (<~80 K) are reasonably well fit by

$$Y_s(E, \theta) = [a_1\alpha(m_i)S_n(E) + \eta(v)S_e(E)^2]/\cos\theta^{(1+x)} \quad (1a)$$

where θ is the angle of incidence measured from the surface normal. The angular term enhances the sputtering yield for ions with shallow angles of incidence (x ~ 0.3–0.7 depending slowly on ion mass and speed). The parameters a_1, α, η(v), and x for water ice *at low incident ion speed*, v, are available in *Fama et al.* (2008) and are used for common ions near Europa in Fig. 2. At high v, the S_e term dominates and the coefficient η decreases with increasing v due to the increase in the radial distribution of the excitations (*Johnson,* 1990).

Using the dependence of S_e on v, a fit to a large amount of sputtering data over a broad range of energies for normal incidence ($\cos\theta = 1$) has been given (*Johnson et al.,* 2004, Fig. 20.6). This fit, shown by the solid line in Fig. 2, is obtained from

$$Y = 1/(1/Y_{low} + 1/Y_{high}) \quad (1b)$$

where Y_{low} and Y_{high} are fits in two different regimes of ion energies. Both have the form $Y_i = Z^{2.8}C_1[v/Z^{1/3}]^{C_2}$, where v is the ion speed divided by 2.19×10^8 cm s^{-1} (=1 au, the speed of a ground state electron in the Bohr hydrogen

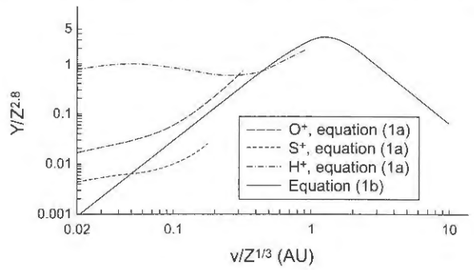

Fig. 2. Sputtering yields of water ice for T < ~100 K as a function of incident ion speed v (divided by 2.19×10^8 cm s^{-1}, or 1 atomic unit of velocity). Solid line: equation (1b), a fit to the data points available at *people.virginia.edu/~rej/sputter_surface.html*. The other lines are low-energy plots of equation (1a) for relevant ions using parameters from *Fama et al.* (2008). Equation (1a) is more accurate than equation (1b) at low ion speeds, where nuclear elastic effects are important.

model) and Z is the number of protons in the incident ion. For Y_{low}, $C_1 = 4.2$ and $C_2 = 2.16$; for Y_{high}, $C_1 = 11.22$ and $C_2 = -2.24$. This fit is most useful when the electronic sputtering effects dominate ($S_e \gg S_n$) and the angular dependence is like that in equation (1a).

Brown and coworkers (e.g., *Brown et al.,* 1982) also showed that the yield was dependent on the ice temperature at T > ~100 K. This dependence is due to the chemistry induced by the incident radiation, a process often referred to as radiolysis (see chapter by Carlson et al.). The primary effect for Europa's atmosphere is the decomposition of ice producing H_2 and O_2. An activation energy, E_a ~ 0.03–0.06 eV, determines the temperature dependence of the decomposition rate, which is also dose dependent at low doses (*Johnson et al.,* 2005). After a minimum dose of ~10^{15} ions/cm^2, during which reactants build up, a rough steady state is achieved (*Reimann et al.,* 1984; *Teolis et al.,* 2005). Using the accumulated database the steady state yield in equivalent H_2O molecules ejected can be written

$$Y(T) \approx Y_s[1 + a_2\exp(-E_a/kT)] \quad (2)$$

For low v ions, a_2 ~ 220 and E_a ~ 0.06 eV (e.g., *Fama et al.,* 2008), for energetic heavy ions relevant to Europa, *Reimann et al.* (1984) find E_a ~ 0.05–0.07 eV (see also *Teolis et al.,* 2005). The production of O_2 is equal to the second term in equation (2), and is roughly half that of H_2. For the ion flux at Europa, the H_2O yield is on the order of 10^9/cm^2 s^{-1} and, due to the effect of the regolith, the O_2 yield is of the same order of magnitude (*Shematovich et al.,* 2005).

Writing the yield in this form is somewhat misleading. Sputtering is a surface ejection phenomena, but the H_2 and O_2 are produced throughout the full penetration depth of the incident radiation. Therefore, the temperature-dependent component of the yield is controlled by diffusion and escape of H_2 and O_2 from the irradiated ice (*Reimann et al.,* 1984; *Teolis et al.,* 2005). O_2 formed at depth is also destroyed by continued irradiation. Therefore, in steady state, production rate is often given as the total number of O_2 produced per 100 eV of energy deposited, called a G-value (see chapter by Carlson et al.). Because the sputtering and decomposition are induced by electronic excitations, incident electrons (*Sieger et al.,* 1998) and UV photons (*Westley et al.,* 1995) also produce gas-phase H_2O, H_2, and O_2. Based on the radiation flux to Europa's surface, the photo-production of volatiles is negligible (a factor of about 10^3 less). For incident electrons, the above expression applies with $S_n = 0$ and α_2 slightly larger because electrons are scattered more efficiently. H, O, and ions are also ejected (*Kimmel and Orlando,* 1995; *Bar-Nun et al.,* 1985), but these yields are typically small.

3.3. Energy Spectra

Modeling of the nearly collisionless atmosphere requires knowing the energies of the ejecta. The few measurements for the steady state yield have been cast in a form typically

used for sputtering. The spectra are given in terms of an effective binding energy, U, and becomes a power law at high energies

$$f(E) = c_q[UE^q/(E + U)^{2+q}]F(E) \quad (3)$$

Here c_q is a normalization constant [such that $\int f(E)\,dE = 1$] and F(E) is a cut-off at large E that depends on the excitation process. In modeling ice sputtering it has been customary to ignore F(E) and use q = 1, c_q = 2, and U = 0.055 eV for the ejection of H_2O, and q = 0, c_q = 1, and U = 0.015 eV for the ejection of O_2 by energetic heavy ions (e.g., *Lanzerotti et al.,* 1983; *Reimann et al.,* 1984; *Shematovich et al.,* 2005). The data used to make these fits is shown in Fig. 3. Although there is prompt ejection of H_2 from the surface layer, most of the H_2 escaping from ice at the relevant temperatures diffuses to the surface and leaves thermally, so that the H_2 is modeled by a thermal flux. In contrast to thermal desorption, equation (3) has a high-energy "tail" proportional to $1/E^2$. Because of this tail, about one-fourth of sputtered H_2O molecules are given enough energy to escape Europa's gravity.

4. ATMOSPHERIC MODELING

4.1. Introduction

Using the data discussed above on the surface composition, radiation flux, and sputtering yields, Europa's atmosphere has been simulated and tested against observations. Species ejected from the surface are tracked analytically or

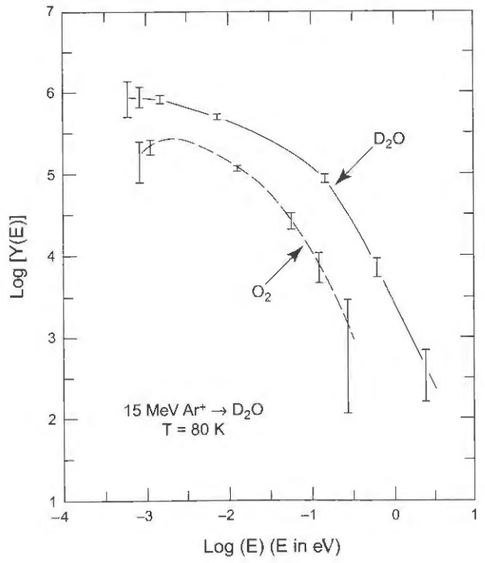

Fig. 3. Laboratory measurements of the energy distribution of sputtered O_2 and D_2O from D_2O ice. From *Lanzerotti et al.* (1983).

numerically along collisionless or more realistic quasi-collisional trajectories taking into account their initial spatial and energy distributions as well as Europa's gravity, photon and electron impact ionization and dissociation, charge exchange, ion-neutral elastic collisions, and interaction with the surface. Jupiter's gravity and solar radiation pressure also need to be considered when modeling the neutral torus.

Sputtering is the dominant source of H_2O, O_2, and H_2, although sublimation of H_2O is competitive at the subsolar point. Atmospheric loss occurs by gravitational escape, interaction with the ambient plasma and UV photons, or removal through interaction with the surface, e.g., the sticking (freezing) of H_2O on Europa's surface. Due to the high-energy tail of the sputtering distribution in equation (3), ejected molecules can have sufficient energy to escape Europa's Hill sphere, the effective limit of Europa's gravitational influence; outside this distance, Jupiter's gravity dominates. The average radius of the Hill sphere is $r_{Hill} \approx a_E\,(m_E/3m_J)^{1/3} = 8.7\,r_E$, where a_E, r_E, m_E, and m_J are Europa's orbital distance from Jupiter's center, Europa's radius, mass, and Jupiter's mass, respectively. Using the energy spectra ahove, ~2% of the O_2 and ~24% of the H_2O are ejected with velocity greater than the 1.9 km/s required to reach r_{Hill}. For thermally accommodated O_2 escape is negligible, but for H_2 about 7% escape at the average temperature (~100 K) and about 15% at the subsolar point (~130 K). These percentages were calculated assuming that molecules do not collide in Europa's atmosphere, for in this nearly collisionless atmosphere, molecules with sufficient energy have a good chance of leaving without encountering another molecule.

Atmospheric neutrals are subject to loss by ionization and charge exchange by the local plasma. Photoionization and dissociation also occur, although at a lower rate (Table 1) (*Shematovich et al.,* 2005; *Smyth and Marconi,* 2006). Ionization or charge exchange followed by pick-up leads to the sweeping of ions from the atmosphere into the magnetosphere or into the surface. Incident plasma ions can also collisionally eject neutrals, often called knock-on or atmospheric sputtering. *Saur et al.* (1998) overestimated this loss process by assuming collisions were head-on (*Shematovich et al.,* 2005). Atomic species formed through dissociation or reactions can also escape. For example, atomic oxygen produced by electron impact dissociation of O_2 is estimated to have, on the average, ~0.67 eV (~2.85 km s^{-1}) of excess energy and likewise H formed from dissociation of H_2 has velocities of several tens of km s^{-1} (*Smyth and Marconi,* 2006); if these atoms are produced isotropically, roughly half will escape.

The rates of the plasma-induced processes depends on temperatures and densities of the charged species. For electron impact ionization and excitation the rate is written $\nu_{ei} = n_e k(T_e)$, where k is a rate coefficient, and n_e and T_e are the electron density and temperature. Important rate coefficients are given in Table 1. The charge exchange rate is $\nu_{chx} \approx \nu_{rel}\,\sigma(\nu_{rel})\,n_i$, where n_i is the ion density. For interactions with the ambient, undisturbed plasma torus ions, the average rela-

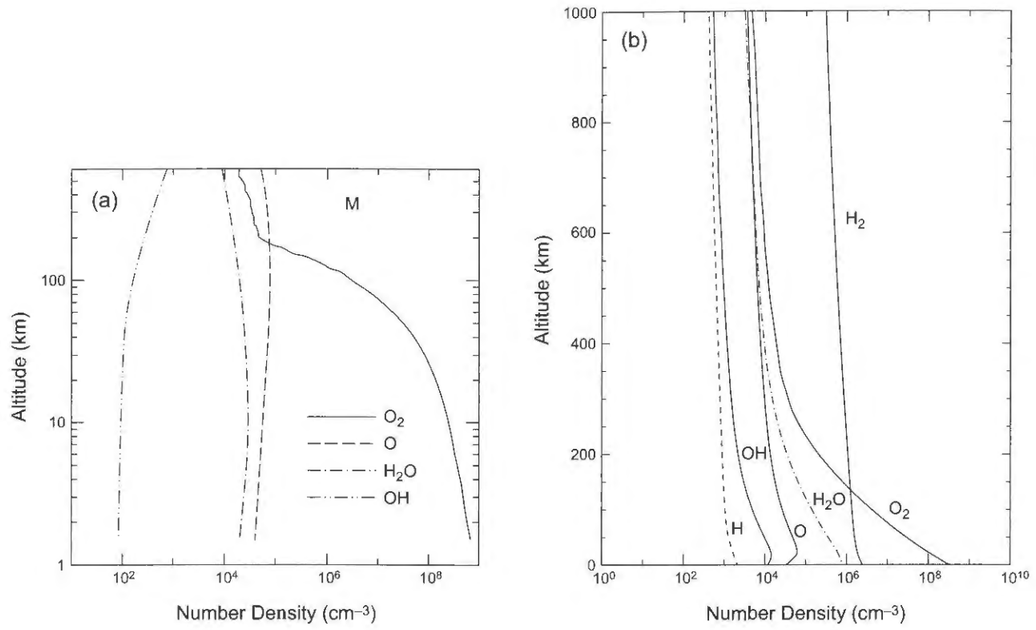

Fig. 4. **(a)** One-dimensional DSMC accounting for photon, electron, and proton impact ionization and dissociation. O and OH are produced by dissociation from O_2 and H_2O; H_2 and H are not included. From *Shematovich et al.* (2005). **(b)** Two-dimensional DSMC globally averaged density. The O_2 rate was set to reproduce the 130.4-nm O brightness of 37 ± 15 Rayleigh observation of *Hall et al.* (1995). Sublimation was taken into account but was unimportant except in the subsolar region. In both simulations, the ejecta energy distributions discussed earlier were used for H_2O and O_2 and thermalization of returning H_2 and O_2 in the regolith is assumed. Sputtering source rates for each model are shown in Table 2. From *Smyth and Marconi* (2006).

tive collision speed is $v_{rel} \approx 10^2$ km/s, the difference between the magnetic field corotation velocity and the Keplerian orbital velocity. In the ionosphere, where the plasma flow velocity is low, v_{chx} is averaged over the ion temperature.

4.2. Analytic Models

For an assumed ballistic atmosphere, analytic expressions are available for calculating the column density, the number of molecules per unit area above Europa's surface (*Johnson,* 1990). Such models were initially used to describe Europa's H_2O and O_2 source and loss rates, including sticking to the surface for H_2O and plasma-induced ionization and dissociation for O_2 (*Johnson et al.,* 1982). The column density of a species, N_i, is

$$N_i \approx (1 - f_i)\Phi_i\tau_i \qquad (4)$$

where Φ_i is the surface source rate given as a flux, f_i is the direct escape fraction, and τ_i is the mean lifetime. For a species like H_2O that sticks to the surface with roughly unit efficiency, τ_i is the ballistic lifetime (~1 hour for bound H_2O). For a species that does not stick, like O_2, $\tau_i^{-1} \approx \nu_i$, the rate for the principal loss process, ionization, which is about six days for O_2. If O_2 is both produced and lost by the ambient plasma, N_{O_2} is *roughly independent* of the plasma density, depending primarily on the local electron temperature, which determines the ionization and dissociation rates (*Johnson et al.,* 1982).

One-dimensional analytic models of the density vs. altitude are also available (e.g., appendix in *Johnson,* 1990). Since O_2 ejected by the incident plasma survives many ballistic hops, it is thermally accommodated to Europa's local surface temperature; i.e., the O_2 desorbs from the surface with a Maxwellian energy distribution. This produces an atmosphere with density that decreases as $\exp[-z/H_{O_2}]$, where z is the height above the surface and $H_{O_2} \approx [kT/m_{O_2}g]$ is called the scale height, with g the gravitational acceleration. For an average temperature of ~100 K, $H_{O_2} \approx 20$ km. Atoms and molecules that do not thermally desorb, such as sodium and H_2O, are sputtered or pbotodesorbed. The energy distribution for sputtering (equation (3)) can be integrated to give the density vs. altitude. In their ionospheric model, *Saur et al.* (1998) assumed that the O_2 atmosphere was primarily escaping and therefore decayed as the square of the distance from the center of Europa. As can be seen in Fig. 4, that would only apply to a fraction of the atmosphere well above ~400 km.

TABLE 2. Sputtering source rates used in Fig. 4.

	Shematovich et al. (2005)	*Smyth and Marconi* (2006)
H_2O	2×10^9 cm^{-2} s^{-1}	3.3×10^9 cm^{-2} s^{-1}
O_2	2×10^9 cm^{-2} s^{-1}	3.3×10^9 cm^{-2} s^{-1}
H_2	—	6.6×10^9 cm^{-2} s^{-1}
H	—	1.9×10^8 cm^{-2} s^{-1}
O	—	1.9×10^8 cm^{-2} s^{-1}
OH	—	1.9×10^8 cm^{-2} s^{-1}

4.3. Monte Carlo Simulations

Monte Carlo simulations are required in order to study the longitudinal and latitudinal morphology and distribution of dissociated fragments. Because of the complexity of the atmospheric origins and the paucity of collisions, two types of Monte Carlo models have been used: a test particle model and a direct simulation Monte Carlo (DSMC) model. In both models atoms and molecules are tracked subject to interactions with the radiation environment and collisions, and are equivalent to solving the Boltzmann equation. In a DSMC simulation one solves for the motion of each particle given the forces and, at each time step, calculates the effect of all possible collisions within Europa's atmosphere and with the incident magnetospheric plasma. Test particle approaches track individual particles in a collisionless atmosphere *or* in a known background atmosphere. If the atmosphere is marginally collisional, a test particle approach can be used iteratively by using a previously calculated atmosphere (background plus test particles) as a background atmosphere in a new calculation. The principal components in Europa's atmosphere have been calculated using one-dimensional DSMC (*Shematovich et al.,* 2005; *Shematovich,* 2006) or two-dimensional DSMC (*Wong et al.,* 2001; *Smyth and Marconi,* 2006) simulations. The three-dimensional structure of Europa's atmosphere and its time variability with respect to its position within Jupiter's magnetosphere have been described using a test particle simulation for sodium (*Johnson et al.,* 2002; *Leblanc et al.,* 2002; 2005; *Burger and Johnson,* 2004; *Cassidy et al.,* 2008). *Ip* (1996) also applied a test particle approach for O_2 in Europa's atmosphere.

5. SIMULATION RESULTS AND COMPARISON TO DATA

5.1. Introduction

McElroy and Yung (1977) predicted that Ganymede would have a robust O_2 atmosphere formed by water sublimation and gas-phase processes. It was later shown that indeed the icy satellites Europa and Ganymede had atmospheres dominated by O_2, but they are tenuous and produced by radiolysis in the icy surface and subsequent sputtering (*Johnson et al.,* 1982). In other words, even if H_2O is the principal ejecta by sublimation and sputtering, these molecules stick to the surface with unit efficiency at the ambient temperature. This is not the case for O_2 molecules, which although formed and ejected less efficiently, have a significantly longer resident time in the atmosphere. The approximate size of the predicted column of O_2 (~10^{15} cm^{-2}) was eventually confirmed by HST observations (*Hall et al.,* 1995).

5.2. One-Dimensional and Two-Dimensional Simulations: Water, Hydrogen and Oxygen Atmosphere

As shown Fig. 4, one-dimensional and two-dimensional DSMC simulations agree on the globally average structure of Europa's atmosphere. Both simulations constrained the O_2 column density to agree with the column density derived from UV emission (*Hall et al.,* 1998). The differences between Figs. 4a and 4b are due to the choice of sputtering rates (shown in Table 2). *Smyth and Marconi* (2006) chose larger ejection rates for O_2 and H_2O and small additional sources of O, OH, H_2, and H directly ejected from the surface. The larger H_2O (near-surface) density in *Smyth and Marconi* (2006) was due to their use of too small a sublimation energy for H_2O. In both simulations the main origin of O and OH is predominantly due to the dissociation of O_2 and H_2O. At the upper altitudes in Fig. 4b, the H_2 decays as ~$r^{-2.8}$ and the O_2 as ~$r^{-3.5}$, roughly consistent with analytic models (*Johnson et al.,* 1990).

Radio occultation measurements were also used to estimate the atmospheric density by assuming an O_2^+ ionosphere that is lost by dissociative recombination (*Kliore et al.,* 1997). They suggested a surface density ~3×10^8 cm^{-3}, consistent with the results in Fig. 4, but with a very different scale height (~120 km). This would give a column density ~4×10^{15}/cm^2, larger than in the models above, in which case the atmosphere would be collisional. However, ions are primarily removed by magnetic field pickup, either away from Europa or into the surface, not by dissociative recombination.

Observations of the O 135.6-nm line indicative of O_2 dissociation displayed a spatially localized emission peak (see chapter by McGrath et al.). Such a feature can be modeled by a spatially nonuniform electron flux and temperature, a spatially nonuniform O_2 atmosphere, or a combination of these. *Cassidy et al.* (2007) first showed that nonuniform O_2 ejection alone could not produce the required density variation as a result of O_2's long lifetime against loss by ionization or dissociation (*Wong et al.,* 2001). However, a

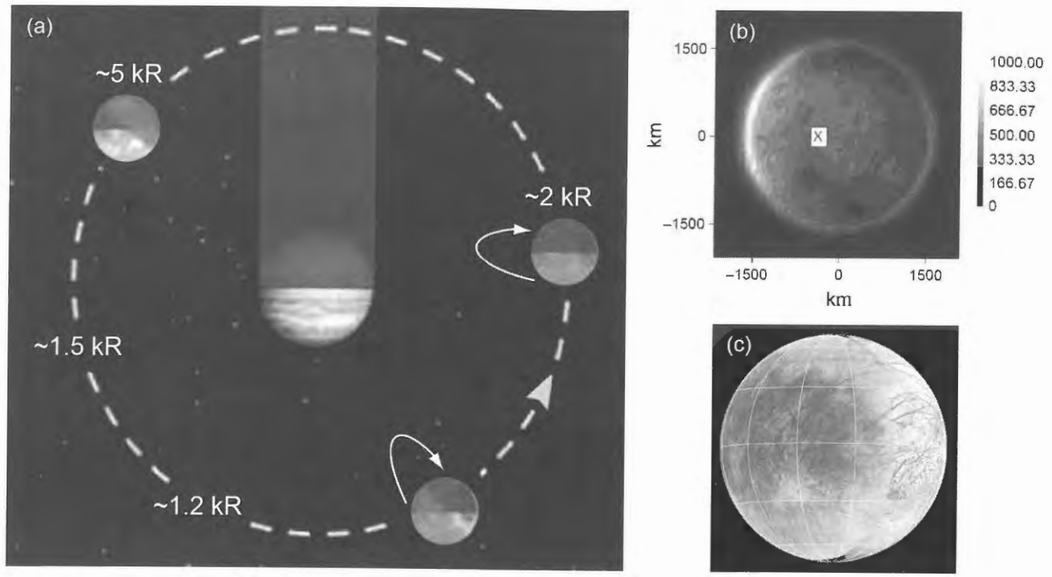

Fig. 5. **(a)** See Plate 25. Average Na emission intensity (in kiloRayleigh) at 4 Europa radii from the surface at different positions around Jupiter (*Leblanc et al.,* 2005). The red part on the surface is the preferentially bombarded trailing hemisphere, whereas the dark part represents the night hemisphere. Also indicated is Jupiter's shadow at Europa's orbit; sizes of Jupiter and Europa are not to scale. White arrows indicate where accumulation of Na atoms on the leading side may occur. **(b)** Simulation of the Cassini observation of Europa in eclipse: brightness in Rayleighs; (x) is apex of trailing hemisphere (*Cassidy et al.,* 2008). **(c)** The surface from the same perspective.

density peak spatially correlated to the observed emission peak could be produced if O_2 is lost via reactions in the regolith in Europa's dark terrain. This terrain has substantial concentrations of sulfur and carbon compounds which may be reactive in a radiation environment. The reactivity was implemented in a test particle model by assigning a probability for a reaction between O_2 and the grains in the dark terrain regolith (*Cassidy et al.,* 2007). This was varied until the spatial distribution of the emission intensity was roughly matched. Because a returning O_2 makes many encounters with grains in the regolith prior to its reentering the atmosphere, the required reaction probability for each encounter with a grain was very small, ranging from 1×10^{-5} to 3×10^{-4}, depending on source and other loss parameters. This small reactivity was sufficient to make a large difference in the atmospheric morphology due to the porous nature of the regolith.

5.3. Trace Species

5.3.1. Sodium atmosphere. Sodium and potassium in Europa's atmosphere have been observed through the resonant scattering of sunlight as discussed. Potassium emission has been only been reported once (*Brown,* 2001), whereas sodium has been observed regularly since its discovery (*Brown and Hill,* 1996; *Brown,* 2001; *Leblanc et al.,* 2002, 2005). Models of the sodium observations have been used to identify the spatial and temporal variability of Europa's extended atmosphere as a function of its orbital position (see Fig. 5a), magnetic longitude, and the angle between the zenith direction and the ram direction of the incident magnetospheric plasma (*Leblanc et al.,* 2002, 2005). A localized emission peak reported by Cassini (*Porco et al.,* 2003) when Europa was in Jupiter's shadow has been associated with sodium preferentially ejected from Europa's dark terrain (*Cassidy et al.,* 2008) (Fig. 5b).

An analytical model (*Johnson,* 2000) was initially used to reproduce the observed vertical distribution of the sodium and to estimate the escape fraction assuming that sodium was carried off with H_2O sputtered from Europa's surface. Comparing source and loss processes, it was suggested that the observed atmospheric sodium is mostly endogenic and therefore could be used as a tracer of Europa's interior composition and, possibly, its putative ocean. *Leblanc et al.* (2002, 2005) developed a three-dimensional test particle simulation of the three-dimensional structure of Europa's sodium atmosphere including its escape component, referred to as the sodium cloud. Sodium was ejected by sputtering (*Johnson et al.,* 2002) and lost by returning to the surface or by ionization. The sputtering rate and its variation with respect to longitude (local time within Jupiter's magnetosphere) and centrifugal latitude (with respect to the Io torus plane) were constrained by observation. Photostimulated and thermal desorption were not included, but their potential effect on the longitudinal variation of the sodium cloud were discussed. Indeed, the content of the extended sodium atmosphere was found to vary by a factor 3 to 4 depending on the orbital position (see Fig. 5a) and again appeared to be primarily endogenic. The significant variation in the sodium density along Europa's orbit was suggested to be due to the variation in the impacting flux of magnetospheric particles, as well as the migration of the sodium atoms from the trailing hemisphere (red portion of Fig. 5a) toward the nightside (dark portion of Fig. 5a), and to their accumulation in a portion of Europa's surface temporarily less irradiated by both photons and energetic particles. This accumulation lasted about a half a Europa orbit until the accumulated sodium was exposed to the solar flux producing the observed emission maximum. This corresponds to the position with an emission of 5 kR in Fig. 5a. *Leblanc et al.* (2002, 2005) also predicted a globally averaged sodium concentration at the surface equal to ~0.01, and suggested that the observed sodium was sputtered from ice and not directly from a mineral or a salt. Recent modeling has improved on this description of the variability and on the Na/K ratios (*Cipriani et al.,* 2008, 2009).

Comparing the simulations to the observations, Europa loses an orbit-averaged flux of $\sim 1.2 \times 10^7$ Na cm^{-2} s^{-1}, about an order of magnitude less than at Io (*Leblanc et al.,* 2005). Since Europa receives a flux of ~0.2 to 0.8×10^7 Na cm^2 s^{-1} from the Io torus, the observed sodium atoms are either endogenic or were implanted in epochs when Io was much more active. The endogenic nature of Europa sodium is also suggested by the significant difference of the Na/K ratios at Europa (25 ± 3) and at Io ($\sim 10 \pm 3$) (*Brown,* 2001; chapter by Carlson et al.). Since a sodium atom has 30% higher escape probability than a potassium atom, the Na/K ratio $\sim 25 \pm 3$ observed far from Europa by *Brown* (2001) implies a Na/K ratio of 20 ± 4 at Europa surface (*Johnson et al.,* 2002). Meteoroid impacts may produce a Na/K ratio of ~13, as measured in meteoroids at Earth, which is still significantly smaller than the required value of 20 ± 4. *Zolotov and Shock* (2001) estimated that the Na/K ratio in the putative internal ocean may be between 14 and 19. Since freezing and dehydration can increase the Na/K ratio, material originating from Europa's ocean that reaches its surface could produce a ratio consistent with that implied by the observations.

5.3.2. Other trace constituents. Both CO_2 and SO_2 have been observed trapped in Europa's surface with apparently different hemispherical distributions, as described earlier. In addition, the surface contains concomitant sulfates and carbonates, molecules with sulfur-sulfur and carbon-carbon bonds, radiation products such as H_2O_2, ion implantation from the Io torus, as well as other endogenic and delivered materials. Because CO_2, CO, SO_2, and SO are more volatile than sodium they should be present in the atmosphere in greater amounts than sodium (*Cassidy et al.,* 2009). However, there is less modeling of the atmospheric content of trace species other than sodium, because of the lack of observations.

Although the sputtering yields of trace species in an ice matrix have not been measured, trace species should be carried away with the large number of water molecules ejected by energetic heavy ions, up to 1000 H_2O ejected per ion. Modeling these trace components requires knowledge of their concentrations in the surface, spatial distribution, and interactions with the surface. The abundance and spatial distribution of a species can be estimated from spectral images (see chapter by Carlson et al.). Assuming ejection is due to the large sputtering yields and the flux of sputtered H_2O is dominated by energetic heavy ion sputtering, then the sputtering rate is nearly independent of latitude and longitude due to large magnetic gyroradii (shown schematically in Fig. 1) (*Cooper et al.,* 2001; chapter by Paranicas et al.). In this approximation, the flux of a trace species will be proportional to its concentration in the surface.

The energy distribution of an ejected trace species is uncertain, but can be approximated by considering that it is ejected along with the H_2O. Assuming that the sodium atoms have the same energy distribution as sputtered H_2O molecules results in a reasonable fit to the sodium data as discussed above. *Wiens et al.* (1998) measured the energy distribution of molecules sputtered from a sodium sulfate solid, one of several candidates for the widespread hydrated substance seen in ice on Europa's surface. They found that the energy distributions for sodium- and sulfur-containing fragments peaked at significantly higher energies than what would be expected for a trace constituent carried off with an H_2O matrix material, *but* with a correspondingly smaller yield. Since any sodium sulfate present on Europa would be hydrated, and in most places is a minor constituent, ejection of trace species with the ice matrix is a reasonable assumption. In regions where the hydrate has a high concentration, ~90% in some places (*Carlson et al.,* 2005), the matrix yield would decrease and the energy of ejecta would increase as the material cohesive energy is larger.

Upon returning to the surface a molecule may "stick" (freeze) or thermally desorb. Modelers have described the probability of sticking as a "sticking coefficient." The closest lab measurement, however, is the residence time on the surface, the average time before thermal desorption. Figure 6 shows the residence time for a variety of species. The temperature range extends from the polar to the subsolar temperatures. The data comes from *Sandford and Allamandola* (1993), except for the O_2 curve from J. Shi (personal communication, 2007). Since there was no data available for SO_2 on H_2O ice, the curve for pure SO_2 was used. It may be appropriate since *Noll et al.* (1995) suggested that SO_2 is segregated from H_2O as inclusions in Europa's surface.

For residence times above the line labeled "lifetime against sputtering," a molecule is more likely to be sputtered before being thermally desorbed. Sodium presumably has a large residence time, but can also be desorbed also by sunlight (*Johnson et al.,* 2002). H_2O_2, sulfur, and other refractory constituents in the ice matrix have large residence times. The residence times for SO_2 and CO_2 cross the sputtering line. For these species, the probability that a molecule will thermally desorb before being sputtered will vary over the europan day. Such a molecule on the nightside is more likely to be sputtered than thermally desorbed, and, when sputtered, will travel much further than a thermally desorbed

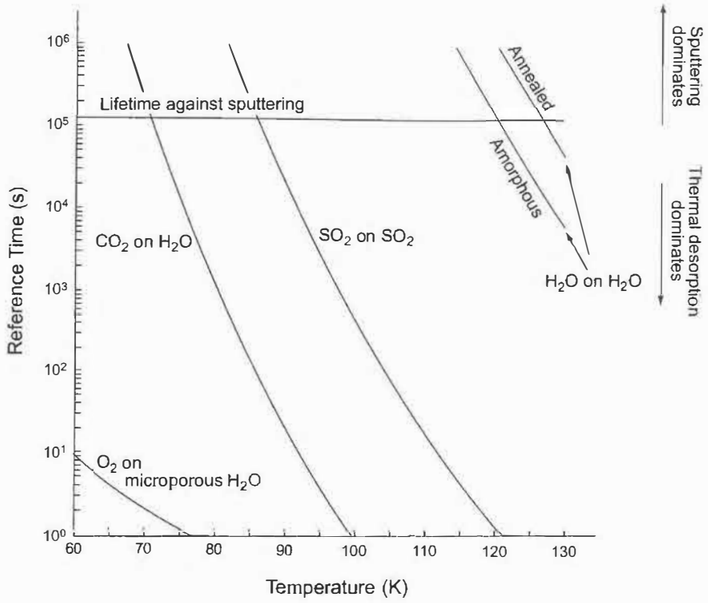

Fig. 6. Residence time vs. temperature. For times above the horizontal line, a molecule is more likely to be sputtered along with H_2O before being thermally desorbed. Data comes from *Sandford and Allamandola* (1993), except for O_2 from J. Shi (personal communication, 2007), and the lifetime against sputtering comes from *Paranicas et al.* (2002).

molecule. Such day-night differences can result in the dynamic redistribution of the atmosphere.

Uncertainties in the residence times are due to lack of data, large error bars, and disagreement between experiments. A potentially larger uncertainty is the porosity of the ice, which has two scales: microporosity or the nanometer scale and regolith porosity on the tens of micrometers scale. Microporous water ice is amorphous and can act like a sponge increasing the residence time by many orders of magnitude (*Raut et al.*, 2007). On the other hand, the time a molecule spends in the regolith due to repeated adsorption and desorption depends sensitively on the thickness of the regolith (*Hodges,* 1980; *Cassidy and Johnson,* 2005; *Cassidy et al.,* 2007). A molecule deep in the regolith can also be protected from sputtering.

6. NEUTRAL CLOUDS AND EXTENDED ATMOSPHERE

Atmospheric molecules can undergo elastic and reactive collisions with the ambient plasma and photochemistry driven by solar radiation. The resulting products will have energy distributions characteristic of their creation and collision processes. Products with sufficient energy can escape the Hill sphere as discussed earlier. Some neutrals, especially those created through charge exchange between plasma ions and atmospheric neutrals, can even escape Jupiter's gravitational field. Most of the escaping particles except H, however, have energies less than Jupiter's escape energy. These constitute the extended atmosphere/neutral cloud as described earlier for sodium. The accumulation of such neutrals, orbiting the planet, is limited by reactions with the magnetospheric plasma and solar radiation. Neutral lifetimes in the magnetosphere are shown in Fig. 7. Neutral lifetimes near Europa are less certain but often assumed to be the same. The morphology and density of the resulting clouds depend upon the interplay of the neutral orbits with the spatially nonuniform magnetospheric plasma and solar radiation. The result is clouds having different morphologies for different species, each containing information about the satellite surface, the ejection process, and the plasma.

Observations of the Europa neutral clouds are limited and include a few observations of the sodium and potassium clouds near Europa, as discussed; a large-scale observation by the Cassini Magnetospheric Imaging Instrument/Ion and Neutral Camera (MIMI/INCA) experiment; and *in situ* plasma measurements. For the sodium and potassium clouds, only that fraction roughly contained in a cylinder located within 40 R_E of Europa has been observed, with a significant fraction contained in the bound component. These observations proved to be highly valuable in defining the source strengths and energy distributions, their variation with time and location on Europa's surface, as well as

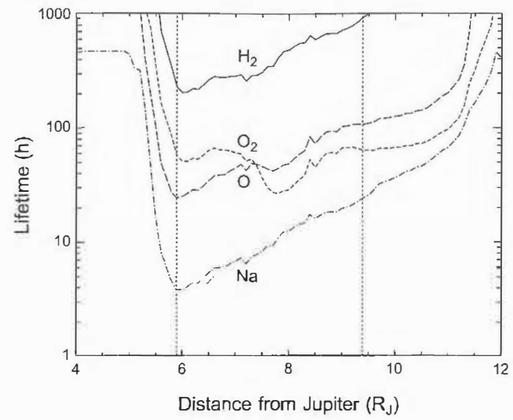

Fig. 7. Mean lifetimes in the equatorial plane of the major neutral cloud species as a function of distance from Jupiter. Updated from *Burger and Johnson* (2004).

the morphology of the local jovian plasma. The Europa sodium cloud is also expected to have a much different morphology from the much-studied Io sodium cloud (*Burger and Johnson,* 2004). As seen in Fig. 8b, the column density was largest in the portion trailing Europa's motion, whereas Io's forward component dominates. This difference is due to the radial morphology of the electron impact ionization lifetime of the sodium, which is determined by the plasma density and temperature. The potassium cloud has been observed and modeled to a far lesser extent (*Brown,* 2001), but is expected to be roughly similar in behavior to sodium after accounting for the larger mass of the potassium atom.

A large-scale, azimuthally averaged observation of the dominant component of Europa's neutral cloud was taken by the ENA imager during the Jupiter Cassini flyby in 2001 (*Mauk et al.,* 2003, 2004). This instrument measures energetic neutrals that are generated by the charge exchange of the energetic component of the plasma with the neutral cloud. Due to the large distance (closest approach ~140 R_J) and one-dimensional nature of the image, little structure was evident, hut two distinct enhancements in the 50–80-keV neutral particle flux were noted just outside the orbit of Europa. Determining the neutral composition causing the enhancements is problematic, but by assuming a torus geometry, *Mauk et al.* (2004) estimated a cloud gas content of $(1.2 \pm 0.5) \times 10^{34}$ for a pure H cloud or $(0.6 \pm 0.25) \times 10^{34}$ for a mixture of water-group gases dominated by H.

Several plasma observations near Europa's orbit are also consistent with the presence of a neutral cloud (*Lagg et al.,* 2003; *Mauk et al.,* 2004). The Galileo energetic particle detector observed an abrupt change in energetic plasma properties with decreasing radial distance upon crossing Europa's orbit. In particular, a drop in energetic plasma density, including the almost complete removal of protons in the tens of keV range (*Paranicas et al.*, 2003; *Mitchell et al.,* 2004), an increase in average energy, and a decrease in the 80–220-keV protons with pitch angle 90° at L = 7.8 R_J (*Lagg et al.,* 2003) were interpreted as being caused by charge exchange with Europa's neutral cloud. Assuming a composition of 20% H and 80% O plus O_2, Lagg et al. estimated the cloud had a density of 20 cm^{-3}–50 cm^{-3}, in agreement with the ENA-derived numbers (*Mauk et al.,* 2003, 2004). Starting with Pioneer 10, plasma measurements near Europa's orbit consistently indicated enhanced oxygen composition and higher temperatures, suggesting the presence of an oxygen neutral cloud (e.g., *Bagenal,* 1994, and references therein).

The neutral cloud observations have stimulated several three-dimensional simulations: sodium (*Leblanc et al.,* 2002. 2005), sodium and O_2 (*Burger and Johnson,* 2004), and O and H_2 (*Smyth and Marconi,* 2006). In each case, the species of interest are initialized with a velocity distribution for the escaping component. Test particles are followed along orbits determined by the gravity of Jupiter and Europa, and, for sodium, solar radiation pressure. For the surface-ejected sodium, *Leblanc et al.* (2002) took into account collisions with the background O_2 atmosphere. The escaped neutrals are destroyed by reactions with the plasma, which is more important than the photoionization. The particles are followed until they collide with Europa or Jupiter, depart the computational domain, or are destroyed by an ion or electron. The model for the plasma that is used to react with the neutral cloud differed somewhat in each study.

For sodium atoms a spatially nonisotropic sputter source with a maximum at the apex of the trailing hemisphere was used (*Leblanc et al.,* 2005) as suggested by albedo variations and by *Pospieszalska and Johnson* (1989). Several energy/angle distributions for f(E,Θ) sputtered sodium were used in the model and the results of each were compared to the data. The model that best matched the data used $f(E,\Theta) \sim [2EU/(E + U)^3]\cos(\Theta)$ with U = 0.055 eV, the energy distribution given above for the large sputtering yields for H_2O carrying off an embedded impurity (*Johnson,* 2000). The excitation and ionization of sodium hy electrons was based on the radial and latitude dependence of plasma electron density given by *Smyth and Combi* (1988). *Burger and Johnson* (2004) calculated a neutral cloud using a spatially isotropic source and an energy distribution similar to *Leblanc et al.* (2002). Their electron model was based on the *Bagenal et al.* (1994) results at the centrifugal equator and assuming an exponential drop in density with magnetic latitude off the centrifugal equator. The model also accounted for an offset dipole and east-west field. For an initial sodium flux of 3×10^7 cm^{-2} s^{-1}, modeled densities are given in Figs. 8a and 8b. Both clouds are concentrated near Europa and exhibit a dominant trailing cloud. However, the cloud in Fig. 8a is significantly more extended due to the use of a lower electron density and thus longer lifetime.

Smyth and Marconi (2006) simulated the O and H_2 neutral clouds. The H_2 atoms were set in motion using the globally averaged H_2 velocity distribution at 1000 km altitude derived from the previously described two-dimensional DSMC atmospheric model. The initial velocity distribution

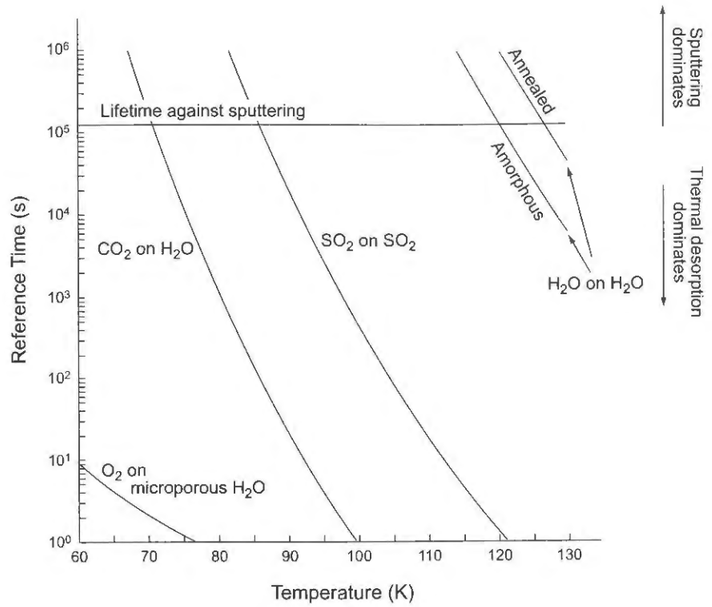

Fig. 6. Residence time vs. temperature. For times above the horizontal line, a molecule is more likely to be sputtered along with H_2O before being thermally desorbed. Data comes from *Sandford and Allamandola* (1993), except for O_2 from J. Shi (personal communication, 2007), and the lifetime against sputtering comes from *Paranicas et al.* (2002).

molecule. Such day-night differences can result in the dynamic redistribution of the atmosphere.

Uncertainties in the residence times are due to lack of data, large error bars, and disagreement between experiments. A potentially larger uncertainty is the porosity of the ice, which has two scales: microporosity or the nanometer scale and regolith porosity on the tens of micrometers scale. Microporous water ice is amorphous and can act like a sponge increasing the residence time by many orders of magnitude (*Raut et al.,* 2007). On the other hand, the time a molecule spends in the regolith due to repeated adsorption and desorption depends sensitively on the thickness of the regolith (*Hodges,* 1980; *Cassidy and Johnson,* 2005; *Cassidy et al.,* 2007). A molecule deep in the regolith can also be protected from sputtering.

6. NEUTRAL CLOUDS AND EXTENDED ATMOSPHERE

Atmospheric molecules can undergo elastic and reactive collisions with the ambient plasma and photochemistry driven by solar radiation. The resulting products will have energy distributions characteristic of their creation and collision processes. Products with sufficient energy can escape the Hill sphere as discussed earlier. Some neutrals, especially those created through charge exchange between plasma ions and atmospheric neutrals, can even escape Jupiter's gravitational field. Most of the escaping particles except H, however, have energies less than Jupiter's escape energy. These constitute the extended atmosphere/neutral cloud as described earlier for sodium. The accumulation of such neutrals, orbiting the planet, is limited by reactions with the magnetospheric plasma and solar radiation. Neutral lifetimes in the magnetosphere are shown in Fig. 7. Neutral lifetimes near Europa are less certain but often assumed to be the same. The morphology and density of the resulting clouds depend upon the interplay of the neutral orbits with the spatially nonuniform magnetospheric plasma and solar radiation. The result is clouds having different morphologies for different species, each containing information about the satellite surface, the ejection process, and the plasma.

Observations of the Europa neutral clouds are limited and include a few observations of the sodium and potassium clouds near Europa, as discussed; a large-scale observation by the Cassini Magnetospheric Imaging Instrument/Ion and Neutral Camera (MIMI/INCA) experiment; and *in situ* plasma measurements. For the sodium and potassium clouds, only that fraction roughly contained in a cylinder located withiu 40 R_E of Europa has been observed, with a significant fraction contained in the bound component. These observations proved to be highly valuable in defining the source strengths and energy distributions, their variation with time and location on Europa's surface, as well as

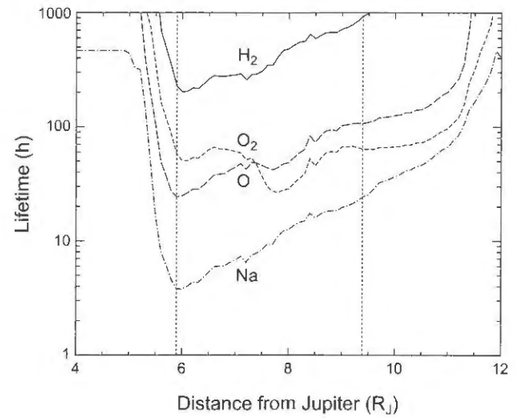

Fig. 7. Mean lifetimes in the equatorial plane of the major neutral cloud species as a function of distance from Jupiter. Updated from *Burger and Johnson* (2004).

the morphology of the local jovian plasma. The Europa sodium cloud is also expected to have a much different morphology from the much-studied Io sodium cloud (*Burger and Johnson,* 2004). As seen in Fig. 8b, the column density was largest in the portion trailing Europa's motion, whereas Io's forward component dominates. This difference is due to the radial morphology of the electron impact ionization lifetime of the sodium, which is determined by the plasma density and temperature. The potassium cloud has been observed and modeled to a far lesser extent (*Brown,* 2001), but is expected to be roughly similar in behavior to sodium after accounting for the larger mass of the potassium atom.

A large-scale, azimuthally averaged observation of the dominant component of Europa's neutral cloud was taken by the ENA imager during the Jupiter Cassini flyby in 2001 (*Mauk et al.,* 2003, 2004). This instrument measures energetic neutrals that are generated by the charge exchange of the energetic component of the plasma with the neutral cloud. Due to the large distance (closest approach ~140 R_J) and one-dimensional nature of the image, little structure was evident, but two distinct enhancements in the 50–80-keV neutral particle flux were noted just outside the orbit of Europa. Determining the neutral composition causing the enhancements is problematic, but by assuming a torus geometry, *Mauk et al.* (2004) estimated a cloud gas content of $(1.2 \pm 0.5) \times 10^{34}$ for a pure H cloud or $(0.6 \pm 0.25) \times 10^{34}$ for a mixture of water-group gases dominated by H.

Several plasma observations near Europa's orbit are also consistent with the presence of a neutral cloud (*Lagg et al.,* 2003; *Mauk et al.,* 2004). The Galileo energetic particle detector observed an abrupt change in energetic plasma properties with decreasing radial distance upon crossing Europa's orbit. In particular, a drop in energetic plasma density, including the almost complete removal of protons in the tens of keV range (*Paranicas et al.,* 2003; *Mitchell et al.,* 2004), an increase in average energy, and a decrease in the 80–220-keV protons with pitch angle 90° at L = 7.8 R_J (*Lagg et al.,* 2003) were interpreted as being caused by charge exchange with Europa's neutral cloud. Assuming a composition of 20% H and 80% O plus O_2, Lagg et al. estimated the cloud had a density of 20 cm^{-3}–50 cm^{-3}, in agreement with the ENA-derived numbers (*Mauk et al.,* 2003, 2004). Starting with Pioneer 10, plasma measurements near Europa's orbit consistently indicated enhanced oxygen composition and higher temperatures, suggesting the presence of an oxygen neutral cloud (e.g., *Bagenal,* 1994, and references therein).

The neutral cloud observations have stimulated several three-dimensional simulations: sodium (*Leblanc et al.,* 2002. 2005), sodium and O_2 (*Burger and Johnson,* 2004), and O and H_2 (*Smyth and Marconi,* 2006). In each case, the species of interest are initialized with a velocity distribution for the escaping component. Test particles are followed along orbits determined by the gravity of Jupiter and Europa, and, for sodium, solar radiation pressure. For the surface-ejected sodium, *Leblanc et al.* (2002) took into account collisions with the background O_2 atmosphere. The escaped neutrals are destroyed by reactions with the plasma, which is more important than the photoionization. The particles are followed until they collide with Europa or Jupiter, depart the computational domain, or are destroyed by an ion or electron. The model for the plasma that is used to react with the neutral cloud differed somewhat in each study.

For sodium atoms a spatially nonisotropic sputter source with a maximum at the apex of the trailing hemisphere was used (*Leblanc et al.,* 2005) as suggested by albedo variations and by *Pospieszalska and Johnson* (1989). Several energy/angle distributions for $f(E,\Theta)$ sputtered sodium were used in the model and the results of each were compared to the data. The model that best matched the data used $f(E,\Theta) \sim [2EU/(E + U)^3]\cos(\Theta)$ with U = 0.055 eV, the energy distribution given above for the large sputtering yields for H_2O carrying off an embedded impurity (*Johnson,* 2000). The excitation and ionization of sodium by electrons was based on the radial and latitude dependence of plasma electron density given by *Smyth and Combi* (1988). *Burger and Johnson* (2004) calculated a neutral cloud using a spatially isotropic source and an energy distribution similar to *Leblanc et al.* (2002). Their electron model was based on the *Bagenal et al.* (1994) results at the centrifugal equator and assuming an exponential drop in density with magnetic latitude off the centrifugal equator. The model also accounted for an offset dipole and east-west field. For an initial sodium flux of 3×10^7 cm^{-2} s^{-1}, modeled densities are giveu in Figs. 8a and 8b. Both clouds are concentrated near Europa and exhibit a dominant trailing cloud. However, the cloud in Fig. 8a is significantly more extended due to the use of a lower electron density and thus longer lifetime.

Smyth and Marconi (2006) simulated the O and H_2 neutral clouds. The H_2 atoms were set in motion using the globally averaged H_2 velocity distribution at 1000 km altitude derived from the previously described two-dimensional DSMC atmospheric model. The initial velocity distribution

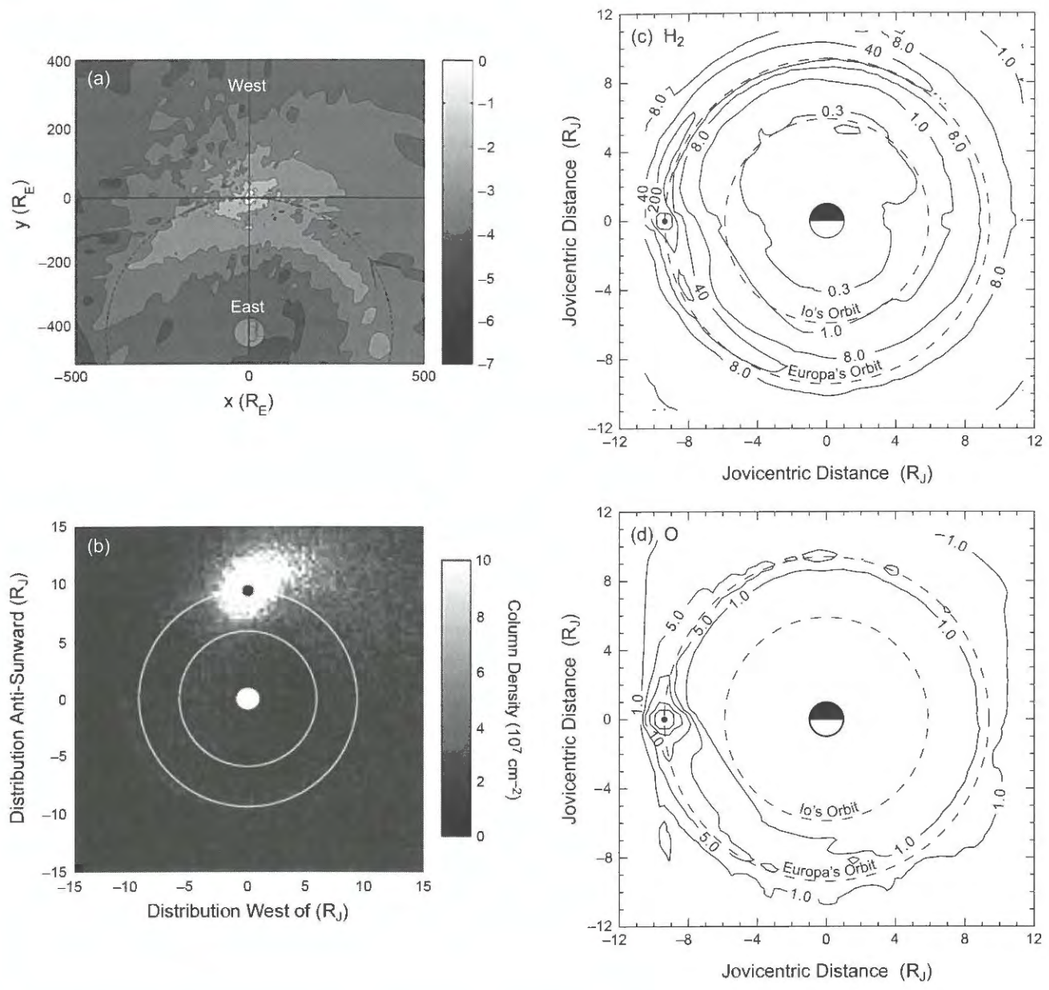

Fig. 8. Neutral cloud (torus) densities or perpendicular column densities viewed from north of the orbit plane with Jupiter in center of each figure. **(a)** Sodium density contours (*Leblanc et al.,* 2002) in a cut centered on Europa's orbit plane at a phase angle of 90°. **(b)** Sodium column density; also roughly the morphology of the O_2 cloud (*Burger and Johnson,* 2004). **(c)** H_2 column density (contour units 1×10^9 cm^{-2}) (*Smyth and Marconi,* 2006). **(d)** Same as **(c)** but for O (contour units 1×10^{10} cm^{-2}).

is a Maxwellian at 120 K with an energetic tail caused by collisions with the fast-moving torus plasma. O atoms were also ejected isotropically, but the energy distribution was, for simplicity, assumed to be monoenergetic with speed 2.5 km s^{-1} (~0.53 eV). Using a velocity distribution for O reduces the escape flux. In the DSMC simulation, the H_2 escape rate was 1.9×10^{27} s^{-1}, while for O, 5.0×10^{26} s^{-1} was used: the sum of the O escape rate and half of the dissociated O_2 (since half of the resulting O atoms likely impact the surface). The plasma model is an update of *Smyth and Combi* (1988) and includes electrons and ions, dipole offset, and east-west field. The plasma density and composition dependence on magnetic latitude is obtained by solving the force-balance equation for the plasma along the field lines. The plasma chemistry includes the electron impact dissociation and ionization of H_2, ionization of O, as well as charge exchange of O with the plasma ions, which dominates atomic oxygen loss within 7 R_J. The results for H_2 and O are shown in Figs. 8c and 8d. The densities are seen to peak near the source, forward and trailing clouds are present, and the neutral cloud is organized about Europa's orbit. The H_2 cloud is broader than the O cloud and both the O and H_2 clouds are more extended than the short-lived sodium cloud (Fig. 7). The neutral clouds for O_2, OH, H_2O, and H were not calculated, but are a smaller fraction of the total since H_2 has, by about an order of magnitude, the highest escape rate. The neutral cloud identified from the EPD and ENA data is likely dominated by H_2 since H is much more dispersed due to the energy acquired during H_2 dissociation.

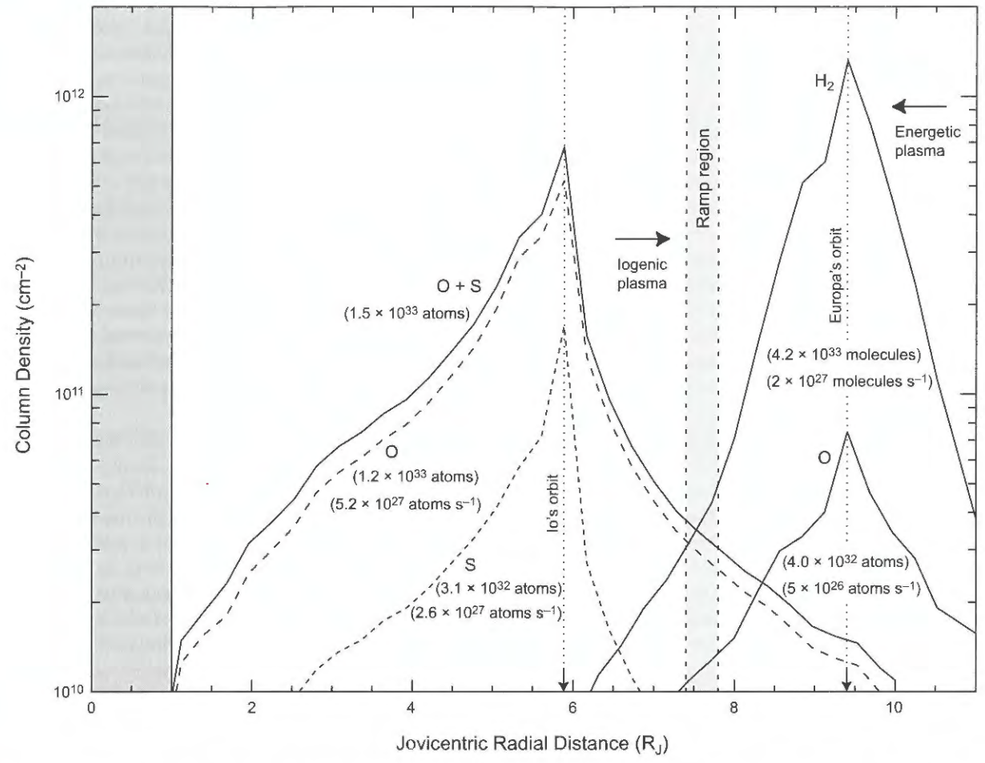

Fig. 9. Comparison of the neutral clouds of Europa and Io. Longitudinally averaged radial column density for Europa's H_2 and O neutral clouds and Io's O, S, and (O + S) clouds (*Smyth and Marconi,* 2006). The total (spatially integrated) cloud population and escape source rate for each neutral cloud as well as the radial location of Jupiter, Io's orbit, and Europa's orbit are indicated.

Europa belongs to a class of satellites, including Io, Enceladus, and Triton, whose neutral clouds contain more matter than their bound atmospheres (*Smyth and Marconi,* 2006). Estimates of the total content of the O and H_2 clouds, 4.0×10^{32} atoms and 4.2×10^{33} atoms respectively, are roughly consistent with the estimates discussed above, but exceed by factors of 1000 and 200 their abundances in Europa's bound atmosphere. The ratio for sodium is smaller due to the shorter lifetime. By comparison the ratio at Io is 3 for O and 1 for S (*Wong and Smyth,* 2000; *Smyth and Marconi,* 2003), and the total Europa neutral cloud content, maximum column density, and maximum density exceed that for the total Io neutral cloud (Fig. 9) by a factor of 3. Although Io is has a much denser atmosphere and a larger source rate, the difference is due to the shorter neutral lifetimes near Io (Fig. 7).

The O and H_2 clouds create a source of plasma, primarily H_2^+, with a net mass loading rate of 22–27 kg s^{-1} (*Smyth and Marconi,* 2006). It peaks near Europa's orbit and is about 10% of Io's total contribution, but exceeds the Io source beyond 8 R_J. Although it is not yet clear in what way this source affects the bulk plasma, it has a significant effect on the energetic particles (*Mauk et al.,* 2004). It depletes the energetic plasma, particularly the proton component, alters the pitch angle distribution and characteristic energy, possibly alters the charge state, and is the primary source of the energetic protons.

In much earlier work, *Schreier et al.* (1993) calculated orbitally averaged densities for H_2O, O_2, H_2, OH, O, and H using a box model that accounted for a large number of reactions between ions and neutrals and a neutral sputtering rate. They predicted that Europa's sputtered products would lead to an enhancement in the oxygen ion composition near its orbit, consistent with observations (*Bagenal,* 1994). While they obtained average densities comparable to those given above, they predicted H rather than H_2 to be the densest neutral cloud. This difference with the more recent models described above is due to the use of different sputtering yields and neglect of escape dynamics and neutral transport.

7. IONOSPHERE MODELING

Both solar radiation and torus plasma ionize atoms and molecules in Europa's atmosphere, as discussed, resulting in an ionosphere. Ions sputtered from the surface are a very small source, but may contribute unique ions. The most abundant ionospheric constituent at lower altitudes is likely O_2^+. Thermal electrons from the magnetosphere (temperature ~20 eV) are primarily responsible for the formation of O_2^+ ions from the dominant O_2 atmosphere. Each ionization event is accompanied by the formation of a cold (~0.5 eV) electron (an "ionospheric electron"). This cold ionospheric electron population is one of three electron populations near Europa, in addition to the thermal (~20 eV) magnetospheric electron population and the nonthermal (or "hot") magnetospheric electron population (sometimes approximated as having a temperature ~250 eV). The thermal magnetospheric population is the most important in determining the lifetime of a molecule against ionization (e.g., Table 1). The cold population doesn't contribute to ionization and the nonthermal population is extremely sparse (*Saur et al.,* 1998; *Schilling et al.,* 2007). The cold ionospheric population is, however, the primary population that contributes to dissociative recombination (e.g., $O_2^+ + e \rightarrow O + O$).

At higher altitudes H_2 is more abundant (Fig. 4b) so that H_2^+ may be expected to dominate for some altitude range until the atmosphere is sufficiently tenuous and the magnetospheric ions dominate. Transport of plasma into the surface and out of the atmosphere limits the accumulation of plasma, as does, to a lesser extent, dissociative recombination of the ionospheric ions. The ionosphere of Europa, unlike ionospheres formed in an atmosphere threaded with closed magnetic field lines or a dense atmosphere, such as Earth and Mars, is continuously lost to the plasma torus on a timescale of minutes. As a result, the ionosphere is expected to be rapidly responsive to changes in torus properties. In addition, due to solar radiation and the histories of the flux tubes intercepting Europa, a dynamic and anisotropic ionosphere that feeds europagenic ions into the plasma torus is expected.

Although Europa's ionosphere has been observed by the Galileo spacecraft (section 2.1 above), there have been few efforts modeling the ionosphere. *Saur et al.* (1998) calculated the electron density in Europa's atmosphere. Using a model for the electric and magnetic fields for a magnetized flow interacting with a satellite developed by *Wolf-Gladrow et al.* (1987) they developed a three-dimensional plasma-neutral interaction model for a constant magnetic field. Although more recent models (*Shematovich et al.,* 2005; *Smyth and Maconi,* 2006) predict a bound O_2 atmosphere with a scale height of 20 km near the surface, the neutral atmosphere was assumed to be O_2 with a r^{-2} height dependence. They also chose an O_2 surface density that varied from the trailing to leading hemisphere as prescribed by *Pospieszalska and Johnson* (1989), in contradiction to later estimates of a more uniform production of O_2. Charge exchange and ion-neutral elastic collisions for the ions and electron impact ionization, dissociation, excitation, and recombination for the electrons were taken into account. As mentioned above, they likely overestimated the atmospheric sputtering rate. The electron density and temperature were calculated for a model with a column of 5×10^{14} cm^{-2} and depletion scale height of 145 km, the result of constraining the model to match the oxygen line brightnesses (*Hall et al.,* 1998). The calculated electron density in the equatorial plane, shown in Fig. 10, was anisotropic with larger densities on the inside of the flanks, reaching a maximum of about 9000 cm^{-3}, roughly agreeing in magnitude and anisotropy with *Kliore et al.* (1997). These are mostly ionospheric (cold) electrons. In the wake, there were no electrons, a limitation of the model rather than a prediction. They also suggested that atmospheric conductivity could affect the estimate of the induced-dipole signature attributed to a subsurface ocean.

Kabin et al. (1999) and *Liu et al.* (2000) constructed self-consistent MHD models, i.e., the model plasma produces a magnetic field in addition to being affected by it. Unlike *Saur et al.* (1998), they also included the Europa's induced magnetic dipole, which is thought to be generated by a conductive subsurface ocean as a response to its motion relative to Jupiter's magnetic field (*Khurana et al.,* 1998; chapter by Khurana et al.). *Kabin et al.* (1999) and *Liu et al.* (2000) varied Europa's boundary conditions (superconducting sphere vs. absorbing boundary), dipole moment, mass loading rate, and other parameters to find the best fit to Galileo magnetometer data. They found that the ionosphere/magnetosphere interaction makes a significant contribution to the magnetic field perturbation near Europa, but that the

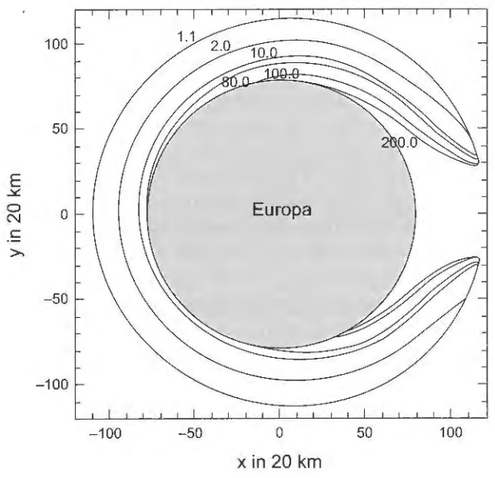

Fig. 10. Model of the density of the equatorial cold electrons density in units of 40 cm^{-3} (*Saur et al.,* 1998). +x is the corotation direction. On the right is Europa's wake, where the electron density is zero in this model.

magnetometer data still requires an induced dipole, such as might be created by a conductive subsurface ocean. Figure 1 shows a schematic of the warped magnetic field near Europa.

Those models used fixed dipoles to approximate Europa's subsurface electromagnetic induction. Most recently, *Schilling et al.* (2007, 2008) modeled the electromagnetic induction self-consistently by including a conductive interior and time-varying magnetic field. In this model, Europa leaves a smaller wake in the magnetospheric plasma than in the models of *Kabin et al.* (1999) and *Liu et al.* (2000). *Schilling et al.* (2008) also predict lower pickup ion densities in the wake than *Kabin et al.* (1999) and *Liu et al.* (2000). This new model wake is in much better agreement with Galileo PLS data (*Paterson et al.,* 1999; chapter by McGrath et al.) than previous models.

8. DETECTION OF EUROPA'S ATMOSPHERE

8.1. Remote Detection

Remote detection is discussed in detail in the chapter by McGrath et al. Even though Earth-based observations of Europa's atmosphere are hampered by the low densities seen in the models and a lack of wavelength coverage, the wealth of likely species suggests that new attempts should be made. Since sodium and potassium are important traces species, continuing observations of the changes in intensity and morphology are important for the modeling of other trace ejecta. The best method for observing the oxygen atmosphere is the FUV O I emission lines at 130.4 nm and 135.6 nm.

8.2. Orbiter: Direct Detection Based on Simulations

The geochemical evolution of the surface and its internal composition are among key objectives of a Europa orbiter. Therefore, *in situ* measurement of Europa's atmosphere, combined with modeling, will give critical compositional information; i.e., from an orbiter placed at 100 km above the surface, trace species should be detectable (*Johnson et al.,* 1998). The 10–100-keV S^+ and O^+ impacting energetic particles act on Europa's surface in a manner similar to the ions beams used in secondary ion mass spectrometry (SIMS), a widely used technique to measure surface composition in the laboratory. SIMS uses a mass spectrometer to measure the ions ejected from the surface. Even though ions are a small fraction of the ejecta they are more readily detected. The yields from Europa's icy surface are large enough to produce a detectable flux of ejected ions, and, as already discussed, the dominant component of ions is produced from neutral atmospheric molecules.

Although the yield from sputtered hydrocarbons is dominated by decomposition products, such as CH_4 and C_2H_x if organics (e.g., gylcerol, POM, L-Leucine) are present in the ice on Europa's surface, whole molecules can be sputtered into the atmosphere (*Johnson and Sundqvist,* 1992). Characteristic ions would also be ejected: e.g., the sputtering of cysteine produces HCN^+, CO_2^+, and even the whole molecules that are protonated (addition of H^+) (*Benninghoven et al.,* 1987). However, organics in the near-surface region are exposed to UV and particle radiation for many years before being sputtered, and thus will be replaced by stable decomposition products such as CO, HCO, HCN, etc. This chemistry is further complicated by the oxidizing surface; e.g., CO produced by decomposition would likely react in the surface to become CO_2 (*Johnson et al.,* 1998). In spite of such complications, near Europa ion detections to date suggest that the local plasma will be rich in species that are characteristic of the surface composition.

The ion densities vs. altitude were roughly estimated for sputtering of species for which laboratory sputtering data were available (*Johnson et al.,* 1998). For simplicity, the neutral column density of impurity sputter products were each scaled to 1% of the O_2 column density if they were volatiles, such as CO_2 and SO_2, or to 1% of the H_2O column density for refractory species such as salts and organics. Combining these neutral densities with ionization lifetimes, CO_2^+, CO^+, NO^+, N_2^+, CH_4^+, NH_3^+, SO_2^+, $NaSO^+$, and HCO^+ could have densities larger than 10 particles/cm^3 at 100 km from Europa's surface. Since a typical ion spectrometer can measure densities smaller than 10^{-3} cm^{-3} if such trace species are present they should be detectable. Similarly, since a typical neutral spectrometer measures densities larger than 1 cm^{-3}, a neutral mass spectrometer will also be useful. A combination of both neutral and ion spectrometers could therefore provide a useful set of surface-related information. Because ejected ions are immediately picked up and can be driven into the surface on the trailing hemisphere, detailed modeling of the near-surface densities is needed. In this way, a low-altitude orbiter could associate local variation of atmospheric composition and density with surface features. At 100 km in altitude, it is expected that a mass spectrometer should provide a spatial resolution at the surface of the same size.

Europa's bulk composition may be also deduced from *in situ* atmospheric measurement. As for the sodium, where the escape rate was used to derive a surface concentration, it should be possible to derive aspects of Europa's interior composition from the full compliment of ejecta. Such measurements would need to energetically characterize the principal escape processes and the implantation rate of exogenic species. These are feasible using both neutral and ion mass and energy spectrometers.

A hydrated substance has been identified on Europa's surface via IR spectroscopy (e.g., *Spencer et al.,* 2006). *Orlando et al.* (2005) suggested that it as a combination of hydrated salts such as $Na_2SO_4^* \times H_2O$ and $MgSO_4^* \times H_2O$, and the radiolysis product $H_2SO_4^* \times H_2O$ (e.g., *Carlson et al.,* 2002). *Wiens et al.* (1997) sputtered pure (nonhydrated) Na_2SO_4 and identified the neutral products via laser ionization. The dominant sputter product was sodium, accompanied by NaO, NaS, Na_2, Na_2O, etc. They also found an extremely low sputtering yield, 0.1 to 0.2 atoms ejected per

3.5 keV Ar^+. The yield for H_2O at comparable heavy ion energy is about 2 orders of magnitude larger. Such low sputtering yields could not account for the sodium source rate needed to model Europa's sodium cloud, but there have been no similar experiments for $Na_2SO_4^* \times H_2O$. The robust source rate seen for sodium suggests that other components of the unidentified hydrated material would likewise be sputtered in amounts comparable to their abundance. Therefore, the hydrated substance could be identified by a mass spectrometer in orbit.

A combined *in situ* measurement of Europa atmosphere by ion and neutral mass and energy spectrometers would also allow a better interpretation of the surface spectral signatures obtained remotely and from the orbiter. Such a spectrometer would need to cover a mass range of up to 400 amu with a mass resolution (m/Δm) between 800 and 1000 if organics are targeted, and would require a typical sensitivity of around 10^{-3} ions/cm^3 and on the order of 100 neutral/cm^3 (*Cassidy et al.*, 2009). In order to distinguish between plasma ions and locally formed ions, an energy range between thermal energies up to few 100 keV with an energy resolution around 10% is required. For the neutral spectrometer to distinguish between bound and escaping molecules, an energy range between thermal energy up to few tens of eV and an energy resolution around 10% would be required. Such spectrometers are presently being designed.

9. CONCLUSIONS

The intense plasma flux onto Europa's water ice surface creates a thin but detectable atmosphere and ionosphere as well as an extensive neutral cloud. Modeling shows these are rich in species derived from Europa's surface. Heavy ions in the jovian plasma erode the surface ejecting up to ~1000 H_2O molecules per ion and any trace species that may be present in the surface. This robust process can eject even refractory components, as suggested by the observed sodium, which might originate in hydrated sulfate salts. Alone, such salts have relatively small sputtering yields, but imbedded in an ice matrix identifiable components are readily ejected by the incident heavy ions. Therefore, most trace species in the surface will be present in the bound and extended atmosphere in some form, so that a sensitive ion and/or neutral mass spectrometer in orbit around Europa would be able to identify many of the surface components.

The incident plasma ions and electrons also break chemical bonds, which then can recombine to form new substances, a process called radiolysis. This produces the O_2 trapped in the surface and that dominates the near-surface atmosphere, as shown by modeling and confirmed by recent Cassini observations. That is, although H_2O is the dominant ejecta it sticks efficiently to surface grains while O_2 does not. Recent modeling shows that O_2 eventually reacts in the regolith or is destroyed (dissociated or ionized and swept away) by the magnetospheric plasma or solar photons. Such interactions are also responsible for the complexity of Europa's ionosphere.

Along with every O_2 created by radiolysis, in steady state two H_2 molecules are also created. These molecules more readily escape Europa's surface material and its gravity to form the most abundant component of Europa's neutral gas cloud, a cloud that, models and observations suggest, contains 10× as many atoms and molecules as Europa's bound atmosphere and possibly more than Io's neutral cloud. This cloud strongly depletes the inward diffusing energetic plasma and is a source of fast H atoms and protons for the magnetosphere. Europa's cloud is, nonetheless, harder to detect by remote sensing than Io's neutral cloud, but a minor component, sodium, has been studied extensively. The modeling results, along with the observations of the less-abundant potassium, have supported the tentative conclusion that Europa's sputtered sodium may be endogenic. Because this result, if proven to be correct, has implications for the presence of an ocean, further alkali observations and concomitant modeling are needed. In addition, *in situ* and remote observations should reveal the presence of many more species as suggested by the modeling described above and by the Galileo measurements of the ion environment. Since those neutrals that are ionized near Europa provide a readily detectable plasma source, we expect a rich ion environment both close to Europa and in the jovian magnetosphere near Europa's orbit.

The modeling described above has shown that the atmospheric structure is complex, but appears to correctly describe the available observations of the oxygen, hydrogen, and sodium content of Europa's gravitationally bound atmosphere and neutral clouds. Based on the physics and chemistry in these models, there is now a critical need for detailed modeling of the desorption of other important trace surface constituents, and for correctly modeling the ionosphere, which is spatially and temporally variable. Such efforts, however, will require a more accurate description of the magnetosphere/satellite interactions, as discussed in the chapter by Kivelson et al., a project that is critically important for the planning of a Europa mission.

REFERENCES

Bagenal F. (1994) Empirical model of the Io plasma torus: Voyager measurements. *J. Geophys. Res., 99,* 11043–11062.

Baragiola R. A. (2003) Water ice on outer solar system surfaces: Basic properties and radiation effects. *Planet. Space Sci., 51,* 953–961.

Bar-Nun A., Herman G., Rappaport M. L., and Mekler Yu. (1985) Ejection of H_2O, O_2, H_2, and H from water ice by 0.5–6 keV H^+ and Ne^+ ion bombardment. *Surface Sci., 150,* 143–156.

Benninghoven A., Rudenauer F. G., and Werner H. W. (1987) *Secondary Ion Mass Spectrometry.* Wiley, New York.

Brown M. E. (2001) Potassium in Europa's atmosphere. *Icarus, 151,* 190–195.

Brown M. E. and Hill R. E. (1996) Discovery of an extended sodium atmosphere around Europa. *Nature, 380,* 229–231.

Brown W. L., Augustyniak W. M., Simmons E., Marcantonio K. J., Lanzerotti L. J., Johnson R. E., Boring J. W., Reimann C. T., Foti G. and Pirronello V. (1982) Erosion and molecular formation in condensed gas films by electronic energy loss of fast ions. *Nucl. Instrum. Meth., 198,* 1.

Burger M. H. and Johnson R. E. (2004) Europa's neutral cloud: Morphology and comparisons to Io. *Icarus, 171,* 557–560.

Carlson R. W., Anderson M. S., Johnson R. E., Schulman M. B., and Yavrouian A. H. (2002) Sulfuric acid production on Europa: The radiolysis of sulphur in water ice. *Icarus, 157,* 456–463.

Carlson R. W., Anderson M. S., Mehlman R., and Johnson R. E. (2005) Distribution of hydrate on Europa: Further evidence for sulfuric acid hydrate. *Icarus, 177,* 461–471.

Cassidy T. A. and Johnson R. E. (2005) Monte Carlo model of sputtering and other ejection processes within a regolith. *Icarus, 176,* 499–507.

Cassidy T. A., Johnson R. E., McGrath M. A., Wong M. C., and Cooper J. F. (2007) The spatial morphology of Europa's near-surface O_2 atmosphere *Icarus, 191,* 755–764.

Cassidy T. A, Johnson R. E., Geissler P. E., and Leblanc F. (2008) Simulation of Na D emission near Europa during eclipse. *J. Geophys. Res.–Planets, 113,* E02005.

Cassidy T. A., Johnson R. E., and Tucker O. J. (2009) Trace constituents of Europa's atmosphere. *Icarus,* in press.

Cipriani F., Leblanc F., Witasse O., and Johnson R. E. (2008) Sodium recycling at Europa: What do we learn from the sodium cloud variability? *Geophys. Res. Lett., 35,* L19201.

Cipriani F., Leblanc F., Witasse O., and Johnson R. E. (2009) Exospheric signatures of alkalis abundances in Europa's regolith. *Geophys. Res. Lett.,* in press.

Cohen C. M. S., Stone E. C., and Selesnick R. S. (2001) Energetic ion observations in the middle jovian magnetosphere. *J. Geophys. Res., 106,* 29871–29882.

Cooper J. F., Johnson R. E., Mauk B. H., Garrett H. B., and Gehrels H. (2001) Energetic ion and electron irradiation of the icy Galilean satellites. *Icarus, 149,* 133–159.

Cooper P. D., Johnson R. E., and Quickenden T. I. (2003) Hydrogen peroxide dimers and the production of O_2 in icy satellite surfaces. *Icarus, 166,* 444–446.

Cosby P. C. (1993) Electron-impact dissociation of oxygen. *J. Chem. Phys., 98,* 9560.

De La Haye V. (2005) Formation and heating efficiencies in Titan's upper atmosphere: Construction of a coupled Io, neutral and thermal structure model to interpret the first INMS Cassini data. Ph.D. thesis, University of Michigan.

Famá M., Shi J., and Baragiola R. A. (2008) Sputtering of ice by low-energy ions. *Surface Sci., 602,* 156.

Hall D. T., Strobel D. F., Feldman P. D., McGrath M. A., and Weaver H. A. (1995) Detection of an oxygen atmosphere on Jupiter's moon Europa. *Nature, 373,* 677–679.

Hall D. T., Feldman P. D., McGrath M. A., and Strobel D. F. (1998) The far-ultraviolet oxygen airglow of Europa and Ganymede. *Astrophys. J., 499,* 475.

Hand K. P., Chyba C. F., Carlson R. W., and Cooper J. F. (2006) Clathrate hydrates of oxidants in the ice shell of Europa. *Astrobiology, 6(3),* 463–482.

Hansen C. J., Shemansky D. E., and Hendrix A. R. (2005) Cassini UVIS observations of Europa's oxygen atmosphere and torus. *Icarus, 176,* 300–315.

Hodges R. R. (1980) Lunar cold traps and their influence on argon-40. *Proc. Lunar Planet. Sci. Conf. 11th,* pp. 2463–2477.

Ip W.-H. (1996) Europa's oxygen exosphere and its magnetospheric interaction. *Icarus, 120,* 317–325.

Itikawa Y. and Mason N. (2005) Cross sections for electron collisions with water molecules. *J. Phys. Chem. Ref. Data, 34,* 1.

Johnson P. V., Kanik I., McConkey J. W., and Tayal S. S. (2005) Collisions of electrons with atomic oxygen: Current status. *Can. J. Phys., 83,* 589–616.

Johnson R. E. (1990) *Energetic Charged Particle Interactions with Atmospheres and Surfaces.* Springer-Verlag, Berlin.

Johnson R. E. (1998) Sputtering and desorption from icy satellite surfaces. In *Solar System Ices* (B. Schmitt and C. deBergh, ed.), pp. 303–334. Kluwer, Dordrecht.

Johnson R. E. (2000) Sodium at Europa. *Icarus, 143,* 429–433.

Johnson R. E. (2001) Surface chemistry in the jovian magnetosphere radiation environment. In *Chemical Dynamics in Extreme Environments, Chapter 8* (R. Dessler, ed.), pp. 390–419. Adv. Ser. Phys. Chem. Vol. 11, World Scientific, Singapore.

Johnson R. E. (2002) Surface boundary layer atmospheres. In *Atmospheres in the Solar System: Comparative Aeronomy* (M. Mendillo et al., eds.), pp. 203–219. AGU Geophysical Monograph 130, Washington, DC.

Johnson R. E. and Jesser W. A. (1997) O_2/O_3 microatmospheres in the surface of Ganymede. *Astrophys. J. Lett., 480,* L79–L82.

Johnson R. E. and Quickenden T. I. (1997) Photolysis and radiolysis of water ice on outer solar system bodies. *J. Geophys. Res., 102,* 10985–10996.

Johnson R. E. and Sundqvist B. U. R. (1992) Electronic sputtering: From atomic physics to continuum mechanics. *Phys. Today, 45(3),* 28–36.

Johnson R. E., Killen R. M., Waite J. H., and Lewis W. S. (1998) Europa's surface composition and sputter-produced ionosphere. *Geophys. Res. Lett., 25,* 3257–3260.

Johnson R. E., Lanzerotti L. J., and Brown W. L. (1982) Planetary applications of ion-induced erosion of condensed-gas frost. *Nucl. Instrum. Meth., 198,* 147–157.

Johnson R. E., Leblanc F., Yakshinskiy B. V., and Madey T. E. (2002) Energy distributions for desorption of sodium and potassium from ice: The Na/K ratio at Europa. *Icarus, 156,* 136–142.

Johnson R. E., Carlson R. W., Cooper J. F., Paranicas C., Moore M. H., and Wong M. C. (2004) Radiation effects on the surface of the Galilean satellites. In *Jupiter: The Planet, Satellites and Magnetosphere* (F. Bagenal et al., eds.), pp. 485–512. Cambridge Univ., Cambridge.

Johnston A. R. and Burrow P. D. (1995) Electron-impact ionization of Na. *Phys. Rev. A, 51,* R1735.

Kabin K., Combi M. R., Gombosi T. I., Nagy A. F., DeZeeuw D. L., and Powell K. G. (1999) On Europa's magnetospheric interaction: A MHD simulation of the E4 flyby. *J. Geophys. Res., 104,* 19983–19992.

Kimmel G. A. and Orlando T. M. (1995) Low-energy (5–120 eV) electron stimulated dissociation of amorphous D_2O ice: $D(^2S)$, $O(^3P)$, and $O(^1D)$ yields and velocity distributions. *Phys. Rev. Lett., 75,* 2606–2609.

Kivelson M. G. (2004) Moon-magnetosphere interactions: A tutorial. *Adv. Space Res., 33,* 2061–2077.

Kliore A. J., Hinson D. P., Flasar F. M., Nagy A. F., and Cravens T. E. (1997) The ionosphere of Europa from Galileo radio occultations. *Science, 277,* 355–358.

Khurana K. K., Kivelson M. G., Stevenson D. J., Schubert G.,

Russell C. T., Walker R. J., and Polanskey C. (1998) Induced magnetic fields as evidence for subsurface oceans in Europa and Callisto. *Nature, 395,* 777.

Kurth W. S., Gurnett D. A., Persoon A. M., Roux A., Bolton S. J., and Alexander C. J. (2001) The plasma wave environment of Europa. *Planet. Space Sci., 49,* 345–363.

Lagg A., Krupp N., Woch J., and Williams D. J. (2003) In-situ observations of a neutral gas torus at Europa. *Geophys. Res. Lett., 30,* DOI: 10.1029/2003GL017214.1556.

Lanzerotti L. J., Maclennan C. G., Brown W. L., Johnson R. E., Barton L. A., Reimann C. T., Garrett J. W., and Boring J. W. (1983) Implications of Voyager data for energetic ion erosion of the icy satellites of Saturn. *J. Geophys., Res. 88,* 8765–8770.

Leblanc F., Johnson R. E., and Brown M. E. (2002) Europa's sodium atmosphere: An ocean source? *Icarus, 159,* 132–144.

Leblanc F., Potter A. E., Killen R. M., and Johnson R. E. (2005) Origins of Europa Na cloud and torus. *Icarus, 178,* 367–385.

Lindsay B. G. and Mangan M. A. (2003) In *Photon and Electron Interactions with Atoms, Molecules and Ions,* pp. 5-1 to 5-77. Londolt-Börnstein Vol. I/17, Subvolume C.

Liu Y., Nagy A. F., Kabin K., Combi M. R., DeZeeuw D. L., Gombosi T. I., and Powell K. G. (2000) Two-species 3D MHD simulation of Europa's interaction with Jupiter's magnetosphere. *Geophys. Res. Lett., 27,* 1791–1794.

Mauk B. H., Mitchell D. G., Paranicas C. P., and Krimigis S. M. (2003) Energetic neutral atoms from a trans-Europa gas torus at Jupiter. *Nature, 421,* 920–922.

Mauk B. H., Mitchell D. G., McEntire R. W., Paranicas C. P., Roelof E. W., Williams D. J., and Krimigis S. M. (2004) Energetic ion characteristics and neutral gas interactions in Jupiter's magnetosphere. *J. Geophys. Res., 109,* A09S12. DOI: 10.1029/2003JA010270.

McCord T. B., Hansen G. B., Fanale F. P., Carlson R. W., Matson D. L., Johnson T. V., Smythe W. D., Crowley J. K., Martin P. D., Ocampo A., Hibbitts C. A., Granahan J. C., and the NIMS Team (1998a) Salts on Europa's surface detected by Galileo's Near Infrared Mapping Spectrometer. *Science, 280,* 1242–1245.

McCord T. B., Hansen G. B., Clark R. N., Martin P. D., Hibbitts C. A., Fanale F. P., Granahan J. C., Segura M., Matson D. L., Johnson T. V., Carlson R. W., Smythe W. D., Danielson G. E., and the NIMS Team (1998b) Non-water-ice constituents in the surface material of the icy Galilean satellites from the Galileo near-infrared mapping spectrometer investigation. *J. Geophys. Res., 103(E4),* 8603–8626.

McCord T. B., Hansen G. B., Matson D. L., Johnson T. V., Crowley J. K., Fanale F. P., Carlson R. W., Smythe W. D., Martin P. D., Hibbitts C. A., Granahan J. C., and Ocampo A. (1999) Hydrated salt minerals on Europa's surface from the Galileo near-infrared mapping spectrometer (NIMS) investigation. *J. Geophys. Res., 104(E5),* 11827–11851.

McCord T. B., Orlando T. M., Teeter G., Hansen G. B., Sieger M. T., Petrik N. G., and Van Keulen L. (2001) Thermal and radiation stability of the hydrated salt minerals epsomite, mirabilite, and natron under Europa environmental conditions. *J. Geophys. Res., 106,* 3311–3319.

McCord T. B., Teeter G., Hansen G. B., Sieger M. T., and Orlando T. M. (2002) Brines exposed to Europa surface conditions. *J. Geophys. Res., 107(E1),* 10.1029/2000JE001453.

McElroy M. B. and Yung Y. L. (1977) Stability of an oxygen atmosphere on Ganymede. *Icarus, 30,* 97–103.

McGrath M. A., Lellouch E., Strobel D. F., Feldman P. D., and Johnson R. E. (2004) Satellite atmospheres. In *Jupiter: Satellites, Atmosphere, Magnetosphere* (F. Bagenal et al., eds.), pp. 457–483. Cambridge Univ., Cambridge.

McKinnon W. B. and Zolensky M. E. (2003) Sulfate content of Europa's ocean and shell: Evolutionary considerations and geological and astrobiological implications. *Astrobiology, 3,* 879–897.

Mitchell D. G., Paranicas C. P., Mauk B. H., Roelof E. C., and Krimigis S. M. (2004) Energetic neutral atoms from Jupiter measured with the Cassini Magnetospheric Imaging Instrument: Time dependence and composition. *J. Geophys. Res., 109,* A09S11. DOI: 10.1029/2003JA010120.

Moncuquet M., Bagenal F., and Meyer-Vernet N. (2002) Latitudinal structure of outer Io plasma torus. *J. Geophys. Res., 107,* A9, 1260. DOI: 10.1029/ 2001JA900124.

Noll K. S., Weaver H. A., and Gonnella A. M. (1995) The albedo spectrum of Europa from 2200 Å to 3300 Å. *J. Geophys. Res., 100,* 19057–19060.

Orlando T. M., McCord T. B., and Grieves G. A. (2005) The chemical nature of Europa surface material and the relation to a subsurface ocean. *Icarus, 177,* 528–533.

Paranicas C., Mauk B. H., Ratliff J. M., Cohen C., and Johnson R. E. (2002) The ion environment near Europa and its role in surface energetics. *Geophys. Res. Lett., 29,* 1074.

Paranicas C., Mauk B. H., McEntire R. W., and Armstrong T. P. (2003) The radiation environment near Io. *Geophys. Res. Lett., 30(18),* 1919, DOI: 10.1029/2003GL017682.

Paterson W. R., Frank L. A., and Ackerson K. L. (1999) Galileo plasma observations at Europa: Ion energy spectra and moments. *J. Geophys. Res., 104,* 22779–22792.

Porco C. C., West R. A., McEwen A., Del Genio A. D., Ingersoll A. P., et al. (2003) Cassini imaging of Jupiter's atmosphere, satellites, and rings. *Science, 299,* 1541–1547.

Pospieszalska M. K. and Johnson R. E. (1989) Magnetospheric ion bombardment profiles of satellites: Europa and Dione. *Icarus, 78,* 1–13.

Raut U, Famá M., Teolis B. D., and Baragiola R. A. (2007) Characterization of porosity in vapor-deposited amorphous solid water from methane adsorption. *J. Chem. Phys., 127,* 204713.

Reimann C. T., Boring J. W., Johnson R. E., Garrett J. W., Farmer K. R., and Brown W. L. (1984) Ion-induced molecular ejection from D_2O ice. *Surface Sci., 147,* 227.

Sandford S. A. and Allamandola L. J. (1993) The condensation and vaporization behavior of ices containing SO_2, H_2S, and CO_2 — Implications for Io. *Icarus, 106,* 478.

Saur J., Strobel D. F., and Neubauer F. M. (1998) Interaction of the jovian magnetosphere with Europa: Constraints on the neutral atmosphere. *J. Geophys. Res., 103,* 19947–19962.

Schenk P. M., Chapman C. R., Zahnle K., and Moore J. M. (2004) Ages and interiors: The cratering record of the Galilean satellites. In *Jupiter: The Planet, Satellites and Magnetosphere* (F. Bagenal et al., eds.), pp. 427–456. Cambridge Univ., New York.

Schilling N, Neubauer F. M., and Saur J. (2007). Time-varying interaction of Europa with the jovian magnetosphere: Constraints on the conductivity of Europa's sub-surface ocean. *Icarus, 192,* 41–55.

Schilling N, Neubauer F. M., and Saur J. (2008) Influence of the internally induced magnetic field on the plasma interaction of Europa. *J. Geophys. Res.–Space Physics, 113,* A03203.

Schreier R., Eviatar A., Vasyliunas V. M., and Richardson J. D. (1993) Modeling the Europa plasma torus. *J. Geophys. Res., 98,* 21231–21243.

Shah M. B., Elliott D. S., and Gilbody H. B. (1987) Pulsed crossed-beam study of the ionisation of atomic hydrogen by electron impact. *J. Phys. B (Atom. Mol. Phys.), 20,* 3501–3514.

Shematovich V. I. (2006) Stochastic models of hot planetary and satellite coronas: Atomic oxygen in Europa's corona. *Solar Sys. Res., 40,* 175–190.

Shematovich V. I., Johnson R. E., Cooper J. F., and Wong M. C. (2005) Surface bound atmosphere of Europa. *Icarus, 173,* 480–498.

Sieger M. T., Simpson W. C., and Orlando T. M. (1998) Production of O_2 on icy satellites by electronic excitation of low-temperature water ice. *Nature, 394,* 554–556.

Smyth W. H. and Combi M. R. (1988) A general model for Io's neutral gas cloud II. Application to the sodium cloud. *Astrophys. J., 328,* 888–918.

Smyth W. H. and Marconi M. L. (2003) Nature of the iogenic plasma source in Jupiter's magnetosphere I. Circumplanetary distribution. *Icarus, 166,* 85–106.

Smyth W. H. and Marconi M. L. (2006) Europa's atmosphere, gas tori, and magnetospheric implications. *Icarus, 181,* 510–526.

Smythe W. D., Carlson R. W., Ocampo A., Matson D., Johnson T. V., McCord T. B., Hansen G. E., Soderblom L. A., and Clark R. N. (1998) Absorption bands in the spectrum of Europa detected by the Galileo NIMS instrument (abstract). In *Lunar and Planetary Science XIX,* Abstract #1532. Lunar and Planetary Institute, Houston (CD-ROM).

Spencer J. R. and Calvin W. M. (2002) Condensed O_2 on Europa and Callisto. *Astron. J., 124,* 3400–3403.

Spencer J. R., Grundy W. M., Dumas C., McCord T. B., Hansen G. B., and Terrile R. J. (2006) The nature of Europa's dark non-ice surface material: Spatially-resolved high spectral resolution spectroscopy from the Keck telescope. *Icarus, 182,* 202–210.

Steffl A. J., Bagenal F., and Stewart A. I. F. (2004) Cassini UVIS observations of the Io plasma torus. II. Radial variations. *Icarus, 172,* 91–103.

Straub H. C., Renault P., Lindsay B. G., Smith K. A., and Stebbings R. F. (1996) Absolute partial cross sections for electron-impact ionization of H_2, N_2, and O_2 from threshold to 1000 eV. *Phys. Rev. A, 54,* 2146–2153.

Teolis B. D., Vidal R. A., Shi J., and Baragiola R. A. (2005) Mechanisms of O_2 sputtering from water ice by keV ions. *Phys. Rev. B, 72,* 245–422.

Volwerk M., Kivelson M. G., and Khurana K. K. (2001) Wave activity in Europa's wake: Implications for ion pickup. *J. Geophys. Res., 106,* 26033–26048.

Westley M. S., Baragiola R. A., Johnson R. E., and Baratta G. A. (1995) Photodesorption from low-temperature water ice in interstellar and circumsolar grains. *Nature, 373,* 405.

Wiens R. C., Burnett D. W., Calaway W. F., Hansen C. S., Lykke K. R., and Pellin M. J. (1997) Sputtering products of sodium sulfate: Implications for Io's surface and for sodium-bearing molecules in the Io torus. *Icarus, 128,* 386–397.

Wiens R. C., Burnett D. S., Calaway W. F., Hansen C. S., Lykke K. R., and Pellin M. J. (1998) Sputtering of sodium sulfate: Implications for Io's surface and sulfur bearing compounds in the Io torus. *Icarus, 128,* 386–397.

Wolf-Gladrow D. A., Neubauer F. M., and Lussem M. (1987) Io's interaction with the plasma torus — A self-consistent model. *J. Geophys. Res., 92,* 9949–9961.

Wong M. C. and Smyth W. H. (2000) Model calculations for Io's atmosphere at eastern and western elongation. *Icarus, 146,* 60–74.

Wong M. C., Carlson R. W., and Johnson R. E. (2001) Model simulations for Europa's atmosphere. *Bull. Am. Astron. Soc., 32,* 1056.

Ziegler J. F., Biersack J. P., and Littmark U. (1985) *The Stopping and Range of Ions in Solids.* Pergamon, New York.

Zolotov M. Y. and Shock E. L. (2001) Composition and stability of salts on the surface of Europa and their oceanic origin. *J. Geophys. Res.–Planets, 106,* 32815–32828.

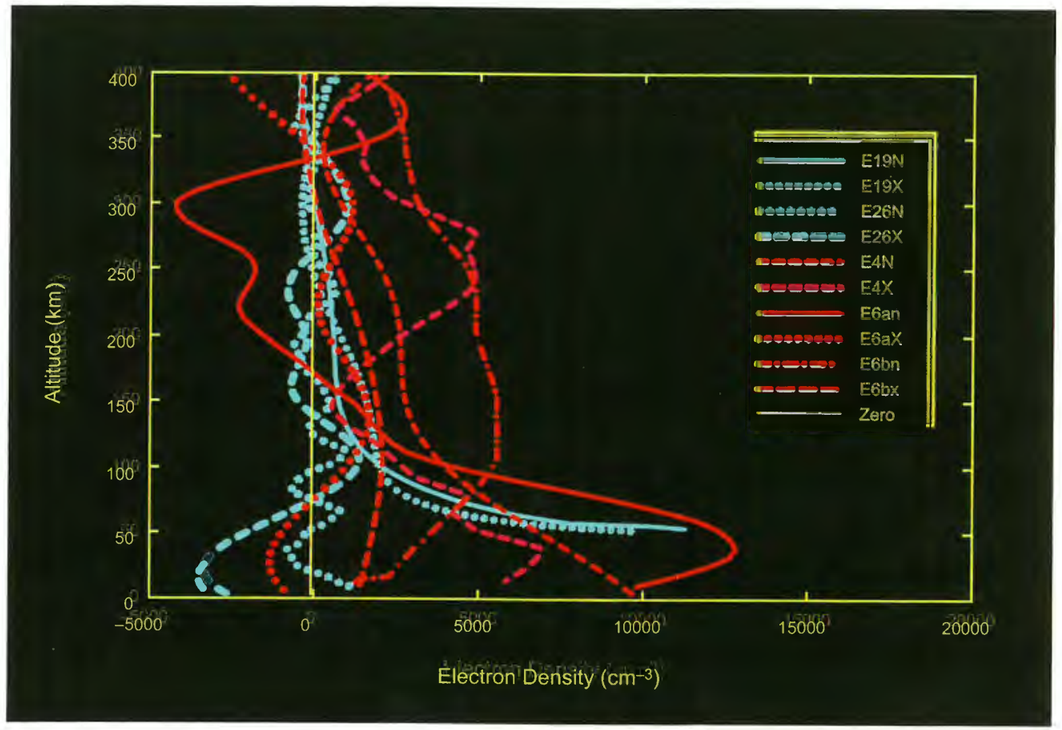

Plate 23. Compilation of all the Galileo radio occultation and near-occultation results illustrating the nonuniformity of Europa's ionosphere. Figure courtesy of A. Kliore.

Accompanies chapter by McGrath et al. (pp. 485–505).

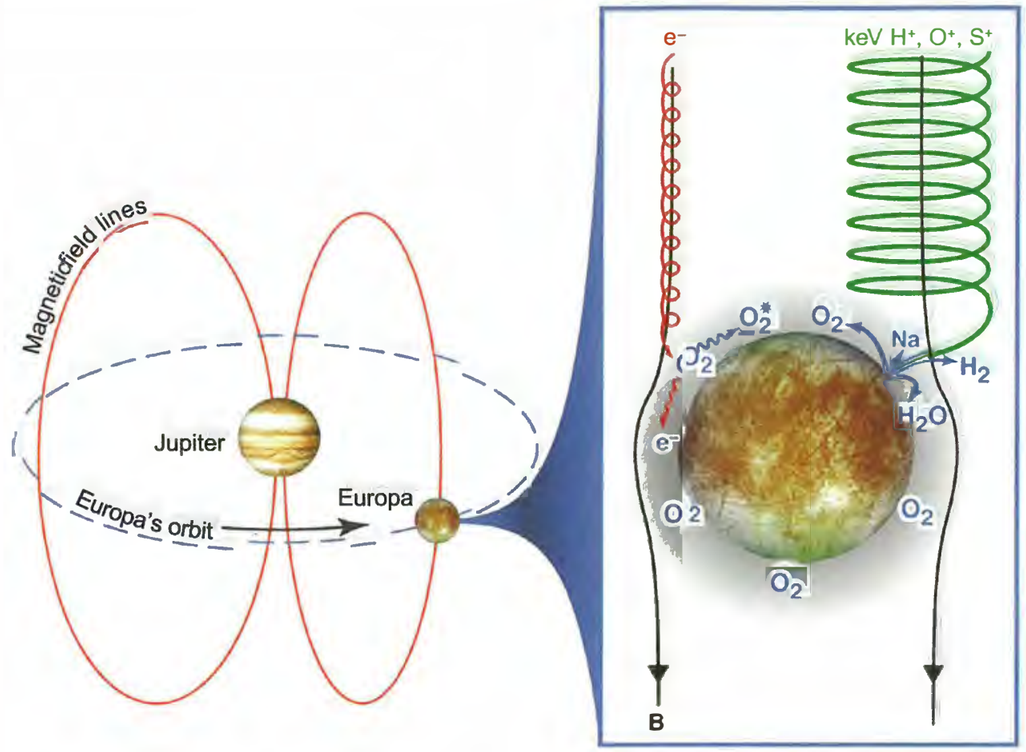

Plate 24. Schematic of Europa's interaction with Jupiter's magnetosphere. Ions and electrons trapped by Jupiter's magnetic field alter and erode the surface, producing a tenuous atmosphere composed mostly of O_2 with an extended neutral torus of primarily H_2.

Accompanies chapter by Johnson et al. (pp. 507–527).

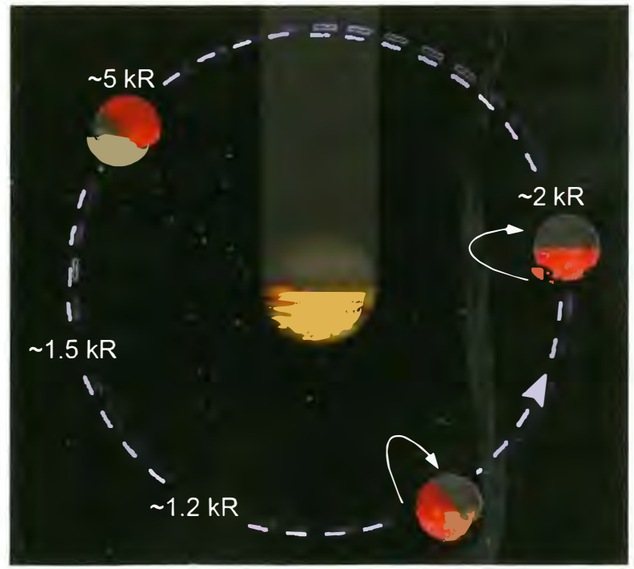

Plate 25. Average Na emission intensity (in kiloRayleigh) at 4 Europa radii from the surface at different positions around Jupiter (*Leblanc et al.*, 2005). The red part on the surface is the preferentially bombarded trailing hemisphere, whereas the dark part represents the night hemisphere. Also indicated is Jupiter's shadow at Europa's orbit; sizes of Jupiter and Europa are not to scale. White arrows indicate where accumulation of Na atoms on the leading side may occur.

Accompanies chapter by Johnson et al. (pp. 507–527).